

IDENTIFICATION OF SCAVENGER RECEPTOR B1 AS THE AIRWAY
MICROFOLD RECEPTOR FOR *MYCOBACTERIUM TUBERCULOSIS*

APPROVED BY SUPERVISORY COMMITTEE

Michael Shiloh, M.D., Ph.D.

Lora Hooper, Ph.D.

Sandra Schmid, Ph.D.

Jennifer Kohler, Ph.D.

David Farrar, Ph.D.

ACKNOWLEDGEMENTS

I would first like to thank my mentor, Dr. Michael Shiloh. I have been lucky to find a mentor as encouraging and brilliant as Dr. Shiloh and I look forward to his continued mentorship as I develop into the physician-scientist he so perfectly exemplifies. I would like to thank my thesis committee for their valuable suggestions and advice. I would finally like to thank my lab mates, both past and present. I have been fortunate to work alongside talented individuals who are willing to lend a helping hand for challenging experiments or just lighten the mood with a well-timed joke. A special thanks goes to Cody Ruhl for always going above and beyond as a lab mate and for being the best bay-mate/friend anyone could ask for.

I would next like to thank my family for their love and support: to my parents, Dr. Abdul Aziz Khan and Dr. Nighat Yasmin, who instilled within me a love of research even in my childhood; to my older siblings, Dr. Nayel Khan and Dr. Saba Shaikh for all of their inspiration and guidance; and to my younger sibling, Dr. Kirin Khan for all of her unwavering support and her beautiful spirit. Finally, I would like to thank my wonderful wife Dr. Gabriella Nguyen, without whom I could not have completed my dissertation.

IDENTIFICATION OF SCAVENGER RECEPTOR B1 AS THE AIRWAY
MICROFOLD RECEPTOR FOR *MYCOBACTERIUM TUBERCULOSIS*

by

HAARIS SUWAID KHAN

DISSERTATION

Presented to the Faculty of the Graduate School of Biomedical Sciences

The University of Texas Southwestern Medical Center at Dallas

In Partial Fulfillment of the Requirements

For the Degree of

DOCTOR OF PHILOSOPHY

The University of Texas Southwestern Medical Center at Dallas

Dallas, Texas
December, 2020

Copyright

by

Haaris Suwaid Khan, 2019

All Rights Reserved

IDENTIFICATION OF SCAVENGER RECEPTOR B1 AS THE AIRWAY
MICROFOLD RECEPTOR FOR *MYCOBACTERIUM TUBERCULOSIS*

Haaris Suwaid Khan, Ph.D.

The University of Texas Southwestern Medical Center at Dallas, 2019

Supervising Professor: Michael U. Shiloh, M.D., Ph.D.

Mycobacterium tuberculosis (Mtb) can enter the body through multiple routes, including via specialized transcytotic cells called microfold cells (M cell). However, the mechanistic basis for M cell entry remains undefined. Here, I show that M cell transcytosis depends on the Mtb Type VII secretion machine and its major virulence factor EsxA. I identify scavenger receptor B1 (SR-B1) as an EsxA receptor on airway M cells. SR-B1 is required for Mtb binding to and translocation across M cells in mouse and human tissue. Together, my data demonstrate a previously undescribed role for Mtb EsxA in mucosal invasion and identify SR-B1 as the airway M cell receptor for Mtb.

TABLE OF CONTENTS

PREFACE	v
TABLE OF CONTENTS	vi
PRIOR PUBLICATIONS	ix
LIST OF FIGURES	x
LIST OF DEFINITIONS	xii
CHAPTER 1: INTRODUCTION AND REVIEW OF THE LITERATURE	1
Introduction	1
Current paradigm of Mtb infection	1
Evidence for Mtb infection of lymphatic tissue	3
Function of mucosa-associated lymphoid tissue	4
Respiratory M cells	6
Macrophage receptors for Mtb uptake	7
Function of Mtb EsxA	8
Concluding remarks	9
CHAPTER 2: MATERIALS AND METHODS	11
CHAPTER 3: T7SS OF MTB IS NECESSARY AND ESXA IS SUFFICIENT TO MEDIATE TRANSLOCATION ACROSS M CELLS	24
INTRODUCTION	24
RESULTS	27
In vitro model of M cell development	27
Mtb T7SS is necessary for translocation across M cells in vitro	29

Mtb T7ss is necessary for binding to M cells in vitro	31
EsxA is sufficient to mediate translocation of inert beads across M cells in vitro.....	34
EsxA binds to the surface of M cells in vitro	36
Expression and purification of recombinant EsxA	38
Recombinant EsxA demonstrates hemolytic, cytolytic, and binding activities	40
EsxA S48A has reduced hemolytic, cytolytic, and binding activities	43
ASB-14 contamination may explain EsxA mediated hemolysis, cytolysis, and binding	45
Mtb T7SS is necessary for translocation across M cells in vivo	47
DISCUSSION	50
CHAPTER 4: IDENTIFICATION OF SR-B1 AS AN ESXA RECEPTOR REQUIRED FOR MTB BINDING AND TRANSLOCATION	51
INTRODUCTION	51
RESULTS	52
Survival based CRISPR screen did not identify an EsxA receptor	52
TriCEPS screen identifies SR-B1 and ApoE as potential EsxA receptors ...	53
EsxA interacts with SR-B1 on both HBE and Caco-2 cells	57
SR-B1 is preferentially expressed by M cells in vitro	59
Loss of SR-B1 reduces EsxA binding to M cells in vitro	61
Loss of SR-B1 reduces Mtb binding and translocation in vitro	64

DISCUSSION	67
CHAPTER 5: PRIMARY HUMAN AIRWAY M CELLS ARE PORTALS OF ENTRY FOR MTB IN A T7SS DEPENDENT MANNER	68
INTRODUCTION	68
RESULTS	68
SR-B1 is expressed preferentially by mouse and human airway M cells in vivo	68
M cells from explanted human adenoids can be identified using flow cytometry	71
Primary human airway M cells have higher SR-B1 expression than neighboring epithelial cells	73
Primary human airway M cells are a portal of entry for Mtb ex vivo	76
Uptake of Mtb by primary human airway M cells depends upon the Mtb T7SS	79
DISCUSSION	80
CHAPTER 6: CONCLUSIONS AND RECOMMENDATIONS	81
SUMMARY OF RESEARCH FINDINGS	81
FUTURE DIRECTIONS	85
BIBLIOGRAPHY	88

PRIOR PUBLICATIONS

Flaherty DP, Harris MT, Schroeder CE, **Khan H**, Kahney EW, Hackler AL, Patrick SL, Weiner WS, Aube J, Sharlow ER, Morris JC, Golden JE. Optimization and Evaluation of Antiparasitic Benzamidobenzoic Acids as Inhibitors of Kinetoplastid Hexokinase 1. *ChemMedChem*. 2017. 12(23):1994-2005.

Nair VR, Franco LH, Zacharia VM, **Khan HS**, Stamm CE, You W, Marciano DK, Yagita H, Levine B, Shiloh MU. Microfold Cells Actively Translocate *Mycobacterium tuberculosis* to Initiate Infection. *Cell Rep*. 2016. 16(5): 1253-58.

LIST OF FIGURES

FIGURE 1. MODEL OF MTB ESX-1 SECRETION SYSTEM	26
FIGURE 2. MODEL OF IN VITRO M CELL DEVELOPMENT	28
FIGURE 3. LOSS OF T7SS REDUCES ABILITY OF MTB TO TRANSLOCATE ACROSS M CELLS IN VITRO.....	30
FIGURE 4. LOSS OF T7SS REDUCES ABILITY OF MTB TO BIND TO M CELLS IN VITRO.....	30
FIGURE 5. ESXA IS SUFFICIENT TO MEDIATE TRANSLOCATION OF INERT BEADS ACROSS M CELLS IN VITRO.....	35
FIGURE 6. ESXA BINDS TO THE SURFACE OF M CELLS IN VITRO	37
FIGURE 7. EXPRESSION AND PURIFICATION OF RECOMBINANT ESXA	39
FIGURE 8. RECOMBINANT ESXA DEMONSTRATES HEMOLYTIC, CYTOLYTIC, AND BINDING ACTIVITIES.....	41
FIGURE 9. ESXA S48A SHOWS A REDUCED HEMOLYTIC, CYTOLYTIC, AND BINDING ACTIVITY.....	44
FIGURE 10. ESXA HEMOLYTIC, CYTOLYTIC, AND BINDING ACTIVITIES MAY BE DUE TO ASB-14	46
FIGURE 11. LOSS OF T7SS REDUCES TRANSLOCATION OF MTB ACROSS M CELLS IN VIVO	49
FIGURE 12. TRICEPS SCREEN IDENTIFIES SR-B1 AND APOE AS POTENTIAL ESXA RECEPTORS.....	55
FIGURE 13. ESXA INTERACTS WITH SR-B1 ON BOTH HBE AND CACO-2	

CELLS	58
FIGURE 14. SR-B1 IS PREFERENTIALLY EXPRESSED BY M CELLS IN VITRO	60
FIGURE 15. LOSS OF SR-B1 REDUCES ESXA BINDING TO M CELLS IN VITRO	62
FIGURE 16. LOSS OF SR-B1 REDUCES MTB BINDING AND TRANSLOCATION IN VITRO	65
FIGURE 17. SR-B1 IS EXPRESSED PREFERENTIALLY BY MOSUE AND HUMAN AIRWAY M CELLS IN VIVO	70
FIGURE 18. M CELLS FROM EXPLANTED HUMAN ADENOIDS CAN BE IDENTIFIED USING FLOW CYTOMETRY	72
FIGURE 19. PRIMARY HUMAN AIRWAY M CELLS HAVE HIGHER SR-B1 EXPRESSION AS COMPARED TO OTHER EPITHELIAL CELLS	74
FIGURE 20. PRIMARY HUMAN AIRWAY M CELLS ARE A PORTAL OF ENTRY FOR MTB EX VIVO	77

LIST OF DEFINITIONS

Mtb – *Mycobacterium tuberculosis*

TB – tuberculosis

M cells – microfold cells

M. bovis – *Mycobacterium bovis*

MALT – mucosa-associated lymphoid tissue

GP2 – glycoprotein 2

PrP^C – cellular prion protein

NALT – nasopharynx-associated lymphoid tissue

BALT – bronchus-associated lymphoid tissue

iBALT – inducible bronchus-associated lymphoid tissue

SR-B1 – scavenger receptor class B type I

EsxA – early secreted antigenic target-6kDa or ESAT-6

RD1 – region of difference-1

T7SS – type VII secretion system

TEER – transepithelial electrical resistance

RBC – red blood cell

CRISPR – clustered regularly interspaced short palindromic regions

ApoE – apolipoprotein E

CHAPTER ONE

Introduction and Review of the Literature

Introduction

Mycobacterium tuberculosis (Mtb) is the causative agent of tuberculosis (TB), the current leading cause of death from a single infectious agent per year [1]. It is estimated that approximately one-third of the world's population has been infected with Mtb and that approximately 1.6 million people died from Mtb infection in 2017 [1], highlighting the on-going need to better understand the biology of Mtb in order to develop novel therapeutic or vaccination strategies to combat this global disease. To survive within the host, Mtb must first cross the epithelial barrier and initiate an infection and herein I focus on the relatively novel interaction between Mtb and specialized epithelial cells known as microfold cells (M cells). I first discuss the current paradigm for how Mtb initiates an infection and describe some shortfalls of this model. I discuss aspects of the host lymphatic system, particularly the mucosa-associated lymphoid tissue and M cells, as it relates to general immunological function and Mtb infection in particular. I finally discuss host receptors and bacterial effectors required for bacterial uptake and highlight the role of Mtb EsxA as a key virulence factor for Mtb.

Current paradigm of Mtb infection

The current paradigm of disease transmission is that an actively infected person produces an infectious aerosol through coughing or sneezing. The size of these aerosols can vary, ranging from less than a micron to over 7 microns in diameter [2]. While several characteristics of these aerosols are relevant to disease outcome, aerosol size is particularly significant as aerosols larger than 5 microns are more likely to be trapped and deposited in the upper airway [3]. Smaller particles are able to pass through the respiratory tract and enter the terminal alveoli where they are phagocytosed by alveolar macrophages or resident dendritic cells, in some cases leading to the initiation of an active infection [4]. However, the vast majority of individuals become latently infected with Mtb, a state in which it has been historically considered that Mtb remains dormant within infected cells inside of a granuloma [5] and, in 5-15% of people with latent infection, will progress to active disease, often correlating with a weakening of the immune system [6]. Recent work has challenged the importance of latent infections in the spread of TB and proposes that the majority of new cases of TB in endemic areas are due to newly acquired infections as opposed to reactivation of latent infections [7]. Therefore, a complete understanding of how Mtb is spread and initiates disease may lead to more rapid and effective changes than previously thought.

The current paradigm can explain pulmonary TB, the most common form of active TB where Mtb is mainly found within the lungs, leading to cough, fever, and weight loss [8]. However, this model has not been definitively proven and cannot explain the occurrence of lymphatic tuberculosis that occurs without any clinical evidence of

pulmonary infection. One such example is tuberculous cervical lymphadenopathy, or scrofula, a disease in which TB is found primarily within the cervical lymph nodes [9]. While this may seem a very rare case of active TB, it is important to note that this form of disease accounts for approximately 10% of all new cases and occurs more often in children [10]. Intriguingly, the majority of cases present with no clinical evidence of pulmonary infection [9]. Since the oropharynx and upper airway lymphatic system drains to the cervical lymph nodes, while the lower airway lymphatic system drains to the mediastinal lymph nodes, it is possible for infection of cervical lymph nodes to completely bypass the lower airways, including the lungs.

Evidence for Mtb infection of lymphatic tissue

There is both historical and recent evidence to consider the possibility that Mtb may use the host lymphatic system to initiate infection. Work performed over a century ago demonstrated that viable Mtb could be isolated from lymph nodes of cadavers who died from causes unrelated to infection and who had no clinical evidence of pulmonary tuberculosis prior to death [11]. During the winter of 1929 and spring of 1930, 251 newborn babies at the Lübeck General Hospital were orally inoculated with the BCG vaccine as part of an effort to reduce childhood TB rates [12]. Unfortunately, vials of the vaccine were accidentally contaminated with fully virulent Mtb, leading to over 90% of the children developing TB, the majority of which was lymphatic or oropharyngeal TB rather than pulmonary tuberculosis [12]. This stark

example highlights how the route of infection impacts disease development, an observation that has been repeatedly confirmed when children drink milk contaminated by *Mycobacterium bovis* (*M. bovis*), a closely related species to Mtb that is also able to cause disease in humans [13]. Oral inoculation of children by *M. bovis* has been repeatedly shown to lead to disproportionately higher rates of lymphatic TB [14].

More recent work has also highlighted the association of Mtb with the host lymphatic system. For example, Mtb has been reported to utilize the lymphatic endothelial cells lining lymphatic vessels as a permissive niche in patients with TB [15]. Additionally, Mtb was able to replicate in primary human lymphatic endothelial cells and this ability depended upon the RD1 locus of Mtb [15]. Additional work in macaques has demonstrated that lymph nodes are generally less bactericidal as compared to lung granulomas [16], which may partly explain why some of the first signs of reactivation of latent TB in macaques may occur in thoracic lymph nodes [17]. While this association of Mtb with the host lymphatic system has been observed for centuries, it is less clear how Mtb is able to invade and establish a niche within the lymphatic system and whether this depends upon primary infection of the respiratory system.

Function of mucosa-associated lymphoid tissue

While lymphoid tissue is found throughout the body, one form of lymphoid tissue known as the mucosa-associated lymphoid tissue (MALT) is found specifically lining

mucosal sites around the body, including the gastrointestinal tract, respiratory tract, and urinary tract [18]. Overlying the MALT are found specialized epithelial cells known as microfold cells (M cells) [19]. M cells were first described within the Peyer's patches of the gastrointestinal tract where, unlike neighboring enterocytes, they were observed to lack microvilli on their apical surface and instead be covered in "microfolds" [20]. M cells are highly phagocytic cells that take up luminal material and deliver it to antigen presenting cells found within a specialized basal pocket underneath the M cell [18]. In this way, M cells can facilitate the development of adaptive immune responses to pathogens or infectious material found within the lumen.

Because of the highly transcytotic nature of M cells, pathogens have evolved to use M cells as a portal of entry. For example, *Escherichia coli* and *Salmonella enterica* serovar Typhimurium express the adhesin protein FimH, a component of the type I pili found on the bacterial outer membrane [1]. M cells, unlike other intestinal epithelial cells, specifically express glycoprotein 2 (GP2) [21], which allows for the recognition and uptake of FimH-expressing bacteria. Loss of either host GP2 or bacterial FimH results in reduced bacterial uptake and diminished antigen-specific immune responses [21], highlighting the importance of M cells in the development of an effective immune response. M cells not only express unique receptors as compared to other epithelial cells but also uniquely localize membrane proteins to atypical sites for antigen recognition. For example, β 1-integrin is normally found on the basal membrane of intestinal epithelial cells as part of a heterodimeric collagen

receptor [22]. However, it is re-localized to the apical membrane of gastrointestinal M cells where it functions as a receptor for *Yersinia pseudotuberculosis* [23]. Finally, ubiquitously expressed proteins may also serve as receptors on M cells. For example, the ubiquitously expressed cellular prion protein (PrP^C) is also expressed on the apical surface of M cells [24] where it functions as a receptor for *Brucella abortus* [25], the causative agent of brucellosis.

Respiratory M cells

As mentioned previously, MALT has also been identified within the respiratory tract. For example, the Waldeyer's ring, composed primarily of the palatine tonsils, nasopharyngeal tonsil (also known as the adenoid), and lingual tonsil, make up the majority of the MALT found in the upper respiratory tract of humans [26]. M cells have been identified on the surface of both the palatine tonsils [27] as well as the adenoid [28] by scanning electron microscopy. Analogous to the Waldeyer's ring, the nasopharynx-associated lymphoid tissue (NALT) is found within the rodent respiratory tract. These paired structures are found within the nasal passages and have also been shown to contain M cells capable of translocating bacteria, such as *Salmonella enterica* serovar Typhimurium [29]. Finally, the bronchus-associated lymphoid tissue (BALT) has been identified in some species but its presence in mice and humans under non-infected conditions is controversial [18]. However, inducible bronchus-associated lymphoid tissue (iBALT) can form from exposure to pathogens,

although it is less clear how similar the immune responses generated from iBALT are as compared to other respiratory MALT [30]. As compared to gastrointestinal M cells, the development and receptor expression of respiratory M cells has been less well characterized. Due to their unique locations and exposure to different environmental antigens and microbiota, it is highly likely that surface receptors would differ between anatomical sites, thereby allowing M cells to interact with unique antigens.

Macrophage receptors for Mtb uptake

Regardless of the route of infection, Mtb must be able to bind to and be internalized by host cells to facilitate growth. Due to its complicated cell wall, Mtb expresses many molecules specific to mycobacterial species in addition to the common molecules shared by most bacteria [31], allowing for both specific and general recognition of Mtb. A number of cell surface receptors interact with Mtb, primarily on macrophages and dendritic cells. Macrophage TLR2 interacts with mycobacterial lipoproteins, such as LpqH [32], and lipids, such as lipomannan [33]. Complement receptors such as CR3 are critical for phagocytosis of Mtb by macrophages as loss of CR3 reduced Mtb uptake by 70-80% [34]. Mannose receptors, which only bind virulent strains of Mtb [34], are able to bind lipoarabinomannan and other sugars found on the bacterial surface [35]. Scavenger receptors such as scavenger receptor class B type I (SR-B1) on macrophages have also been reported to bind Mtb,

although the physiological role of this receptor is unclear as there was no difference in bacterial replication or early host survival after SR-B1^{-/-} mice were infected with Mtb via the aerosol route. [36]. Scavenger receptors were also important for uptake of Mtb by mesenchymal stem cells as shRNA mediated knock-down of MARCO and SR-B1 reduced bacterial uptake [37].

Function of Mtb EsxA

While Mtb expresses a number of virulence factors to survive within the host, one of the best characterized virulence proteins expressed by Mtb is EsxA (also known as early secreted antigenic target-6 kDa or ESAT-6). EsxA is secreted as a heterodimer with EsxB through a specialized type VII secretion system known as the ESX-1 system [38]. EsxA and EsxB are part of the region of difference-1 (RD1) locus of Mtb, a segment of DNA lost in the attenuated BCG strain of *M. bovis* [39]. Deletion of RD1 from Mtb leads to attenuation of the bacteria [39] while complementation of the BCG strain with RD1 increases virulence [40], highlighting the importance of this pathway for Mtb virulence.

EsxA performs several functions. For example, EsxA binds to laminin to facilitate invasion of Mtb [41] and beta-2 microglobulin to impede antigen presentation [42]. Additionally, loss of EsxA secretion reduces phagosomal rupture [43] and cytosolic access of Mtb from the phagosome within the macrophage [44]. These observations are in line with the hypothesis that EsxA is a secreted, pore-forming molecule, as

evidenced by the ability of EsxA to lyse red blood cells [45] and type II pneumocytes [41]. However, EsxA has been identified to be present on the bacterial surface [41, 46], the pore-forming ability of EsxA has been recently called into question [47, 48], and recent work has also demonstrated that loss of EsxA and EsxB secretion by Mtb does not always lead to attenuation [49]. This recent shift in the proposed function of EsxA highlights the ongoing need to better understand the role of EsxA in the context of infection.

Concluding remarks

Work by multiple groups has shown that various mycobacterial species may be able to interact with M cells. For example, *Mycobacterium avium* [50] and the BCG strain of *M. bovis* [51] are able to translocate across Peyer's patches. Previous work has identified Mtb within cells with the morphology of M cells [52]. Our lab has recently expanded this work to identify Mtb both on the surface of and inside M cells in vitro [31]. Additionally, loss of M cells in mice prior to infection reduces dissemination of bacteria from the initial site of infection to regional lymph nodes and provides a significant survival advantage to mice as compared to control mice [31], highlighting the role of M cells in the context of Mtb infection in vivo. However, a mechanistic understanding of this process is lacking and it is currently unclear if M cells may be a portal of entry for Mtb in humans. A better understanding of the specific molecules

involved in the initial uptake of Mtb may lead to the development of novel vaccine targets to prevent bacterial uptake and thereby prevent disease.

CHAPTER TWO Methodology

MATERIALS AND METHODS

Bacterial strains and Media

M. tuberculosis Erdman, *M. tuberculosis* Erdman $\Delta eccD1$ [53], *M. tuberculosis* Erdman $\Delta esxA$ [53], *M. tuberculosis* Erdman *cor:Tn7* [31] were grown in Middlebrook 7H9 medium or on Middlebrook 7H11 plates supplemented with 10% oleic acid-albumin-dextrose-catalase. Tween 80 (Fisher T164-500) was added to liquid medium to a final concentration of 0.05%. Culture and growth of cell lines

Cell culture

The human colorectal adenocarcinoma cell line Caco-2 (HTB-37) and human Burkitt lymphoma cell line Raji B (CCL-86) were obtained from ATCC (Manassas, VA, USA). 16HBE14o- cells [47] were provided by Dieter Gruenert (University of California, San Francisco). Caco-2 or HBE cells were grown in DMEM (Gibco 11965092) supplemented with 20% fetal bovine serum (Gibco 26140079), 50 units/mL penicillin (Gibco 15140122), 50 $\mu\text{g}/\text{mL}$ streptomycin (Gibco 15140122), 2 mM L-glutamine (Gibco 25030081), 1% sodium pyruvate (Gibco 11360070), 1% non-essential amino acids (Gibco 11140050), and 1 mM HEPES (Hyclone SH30237.01). Raji B cells were grown in DMEM supplemented with 20% FBS and 2

mM L-glutamine. In order to generate stable knock-down lines of SR-B1 or Dock4, HBE cells were transduced with lentivirus containing the appropriate shRNA cloned into pLKO.1 (Addgene 10878) as described previously [48]. Transduced cells were selected with puromycin (Sigma-Aldrich P8833-10MG) and surviving cells were maintained in puromycin for three additional passages.

Tissue bilayer model

3×10^5 Caco-2 or HBE cells in 1 mL of media were plated in the upper chamber of a 3 μ m transwell insert (Corning 3462). Either 5×10^5 Raji B cells in 2 mL of media or 2 mL of media alone were added to the basal chamber. 1 mL of media in the upper chamber and 1 mL of media in the bottom chamber were aspirated daily and replaced with 1 mL of fresh media. The transwells were maintained at 37°C for 2 weeks or until the transepithelial electrical resistance was greater than 350 Ω .

Tissue bilayer immunofluorescence microscopy

In order to image binding of Mtb to transwells, mCherry Mtb was grown until mid-log phase, washed, and centrifuged and sonicated to remove clumps. Bacterial inoculum was added to the upper chamber of the transwell at a MOI of 5:1 for 2 hours at 4°C with gentle agitation. Transwells were gently washed and fixed with 4% paraformaldehyde in PBS at 4°C for one hour. Transwell inserts were stained with

DAPI (Thermo D1306) and excised using a blade. Transwell inserts were mounted on microscope slides using Prolong Gold antifade reagent (Invitrogen P36390) and imaged using an AxioImager MN microscope (Zeiss). In order to image binding of EsxA to transwells, EsxA was expressed and purified as described. EsxA was then biotinylated by the Sulfo-SBED reagent (Thermo 33033) per manufacturer's instructions and excess reagent was removed via size exclusion columns (GE Healthcare 17-0851-01). Transwells were then incubated with 1.5 μ M EsxA in HBSS for 2 hours at 4°C with gentle agitation, washed, and exposed to UV light for 30 minutes at room temperature to allow for cross-linking. Transwells were then fixed with 4% paraformaldehyde in PBS for 15 minutes at room temperature, blocked with 10% donkey serum (Sigma D9663-10ML) in PBS for three hours at room temperature, and incubated with a 1:100 dilution of rabbit anti-SR-B1 antibody (Abcam 52629) in 2% donkey serum in PBS overnight at 4°C. The following day, transwells were washed and incubated with a 1:100 dilution of PE-conjugated rat NKM 16-2-4 (Milteny 130-102-150), a 1:500 dilution of an AlexaFluor 647 conjugated donkey-anti-rabbit secondary antibody (Thermo A-31573), and a 1:500 dilution of AlexaFluor 488 conjugated streptavidin (Jackson 016-540-084) for 1 hour at room temperature. Transwells were then washed, stained with DAPI, excised with a blade, mounted, and imaged as described.

In vitro Mtb infection

Liquid cultures of Mtb were grown until mid-log phase, washed three times with PBS, and centrifuged and sonicated to remove clumps. Bacteria were then resuspended in DMEM + 20% fetal bovine serum. For translocation assays, bacterial inoculum was added to the upper chamber of the transwell at a MOI of 5:1 and media from the basal compartment was sampled after 60 minutes. The samples were then plated on 7H11 agar plates and maintained in a 37°C incubator for 3 weeks to allow for colony formation. For binding assays, bacterial inoculum was added to the upper chamber of the transwell at a MOI of 5:1 and incubated at 4°C for two hours with gentle agitation. Transwells were gently washed and lysed with 0.5% Triton X-100 (Sigma T8787) and serial dilutions were plated on 7H11 plates. Plates were incubated in a 37°C incubator for 3 weeks to allow for colony formation.

Mouse intranasal infection

Mtb Erdman and all mutants were grown in 7H9 and 0.05% Tween-80 until mid-log phase. Cultures were washed three times with PBS, centrifuged to remove clumps, and sonicated to yield a single-cell suspension. Bacteria were resuspended to yield a final concentration of 1×10^8 bacteria in 10 μ L PBS. BALB/c mice obtained from The Jackson Laboratory were infected with 10 μ L of the bacterial suspension intranasally. NALT from 3-5 mice were collected, homogenized, and plated on 7H11 (Difco 283810) plates supplemented with 10% OADC to enumerate the number of bacteria deposited in the airway on Day 0. Mice were sacrificed on Day 7 post-

infection and cervical lymph nodes were collected, homogenized, and plated on 7H11 plates. Plates were incubated in a 37°C incubator for 3 weeks to allow for colony formation.

Microsphere conjugation and translocation

Microspheres were conjugated to protein as per instructions (Polylink 24350-1). Briefly, 12.5 mg of microspheres were centrifuged and washed twice in coupling buffer. Microspheres were then incubated with an EDAC/coupling buffer solution to activate the microspheres. 200 µg of protein was added to the beads, thereby allowing for covalent binding of the protein to the microspheres. Microspheres were then washed twice with PBS and stored at 4°C. In order to test the ability of these beads to translocate in the tissue bilayer assay, beads were diluted to an MOI of 5:1 in DMEM + 20% fetal bovine serum and added to the apical chamber of transwells. Media from the basal compartment was sampled after 60 minutes and the number of beads present in the sample was analyzed by flow cytometry using an LSR II (BD).

Protein expression and purification

gBlocks (IDT) encoding for EsxA or EsxB from Mtb were obtained and cloned into the pENTR entry vector (Thermo K240020) prior to being cloned into the pDest17 destination vector (Thermo 11803012; Thermo 11791020) per the manufacturer's

protocol. The resulting vector was transformed into the BL21 strain of *E. coli* (NEB C25271) for protein expression. 1 L of bacterial culture was grown to an OD₆₀₀ of 0.6, induced with 1 mM IPTG (Promega V3955) at 37°C for 3 hours, and centrifuged at 3500 rpm for 15 minutes at 4°C to yield a bacterial pellet. The bacterial pellet was then resuspended in 15 mL of resuspension buffer (50 mM sodium phosphate, 500 mM NaCl, pH 7.4) with one tablet of EDTA-free protease inhibitor (Roche 11836170001). Bacteria were lysed by sonication and centrifuged at 11200 rpm for 15 minutes at 4°C. The resulting pellet was resuspended in 20 mL of 8 M urea in resuspension buffer and incubated for 2 hours at room temperature with gentle agitation. The protein slurry was again centrifuged at 11200 rpm for 15 minutes at 4°C and the resulting supernatant was incubated with cobalt TALON affinity resin (Clontech 635503) for 2 hours at room temperature. Resin was washed with 8 M urea in resuspension buffer and EsxA or EsxB was eluted with 150 mM imidazole and 8 M urea in resuspension buffer. The eluate was dialyzed overnight using a Slide-a-Lyzer dialysis cassette (Thermo 66203) against 10 mM ammonium bicarbonate. The dialyzed sample was again incubated with cobalt TALON affinity resin for 2 hours at room temperature. Resin was subsequently washed with 10 mM Tris-HCl pH 8.0, 0.5% ASB-14 (Sigma A1346-1G) in 10 mM Tris-HCl pH 8.0, and 10 mM Tris-HCl pH 8.0. EsxA or EsxB was eluted with 150 mM imidazole in PBS, dialyzed overnight against PBS, and stored at 4°C.

Adherent Binding Assay

10^5 HBE cells were plated in a well of a 96 well plate and allowed to adhere overnight. The following day, Mtb EsxA or Mtb EsxB were added to the wells at increasing concentrations. Plates were incubated at 4°C for two hours, washed, and fixed in 4% paraformaldehyde for 20 minutes. Plates were blocked with 10% donkey serum in PBS for two hours at room temperature and incubated with 1:100 mouse anti-6xHis in 2% donkey serum overnight at 4°C. Plates were washed, incubated with 1:500 HRP-conjugated goat anti-mouse secondary antibody for one hour at room temperature, washed, and incubated with 100 μ L 1-Step Ultra TMB-ELISA substrate (Thermo 34028) for 15 minutes. The reaction was quenched with 100 μ L 2 M sulfuric acid and absorbance was measured at 450 nm.

Cytolysis assay

10^5 HBE cells were plated in a well of a 96 well plate and allowed to adhere overnight. The following day, Mtb EsxA or Mtb EsxB were added to the wells at increasing concentrations. Plates were incubated at 37°C for 24-72 hours. Cell lysis was determined using the Pierce LDH cytotoxicity assay kit (Thermo 88953) per the manufacturer's protocol.

Hemolysis assay

100 μ L of packed sheep red blood cells were washed twice with PBS and incubated with Mtb EsxA, Mtb EsxB, or MBP in PBS at various concentrations for five minutes. Intact RBCs were pelleted and the hemoglobin content in the supernatant was determined by measuring absorbance at 405 nm.

Mutant EsxA construction and purification

EsxA from Mtb was aligned with EsxA from *Mycobacterium smegmatis*, *Mycobacterium leprae*, and *Mycobacterium marinum* using Clustal Omega. Conserved residues were compared against the crystal structure of EsxA from the protein data bank (3FAV) to identify surface exposed residues. gBlocks encoding for substitutions of conserved residues to alanine in Mtb EsxA were ordered from IDT and cloned/purified as described for WT EsxA.

Quantification of ASB-14 contamination

ASB-14 (A1346, Sigma Aldrich) was resuspended in PBS at concentrations ranging from 375 nm to 11.5 mM. ASB-14 standards and purified EsxA in PBS were extracted with 2:1:1 DCIM: MeOH: H₂O (dichloromethane: methanol: water). Extracts were centrifuged and the bottom organic layer was collected. Samples were manually infused with a syringe on quadrupole TOF TripleTOF™ 6600+ mass spectrometer (SCIEX, Framingham, MA). ESI source parameters were as follows:

ion source gas 1 (GS1) and gas 2 (GS2) set to 20 and 15 psi; curtain (Cur) gas set to 25 psi; source temperature of 300°C; and ion-spray voltage of -4,000 V in the positive ionization mode. GS1 and GS2 were zero-grade air, while Cur gas was nitrogen. TOF scans from 100-2000 m/z were collected over 30 seconds with a flow rate of 10 μ L/min. Data were analyzed in PeakView (SCIEX) to look for the presence of ASB-14 monomer (435.4 m/z), dimer (869.8 m/z), and trimer (1304.2 m/z). Prism 7 (GraphPad) was used to generate a standard curve of ASB-14 with associated peak intensity and used to interpolate the quantity of ASB-14 present in 200 μ g of purified EsxA.

CRISPR screen

The Brunello CRISPR library (Addgene 73179) was transformed into MachI *E. coli*. Bacteria were plated on ampicillin containing LB plates and incubated at 30°C overnight. Bacterial colonies were scraped from the plate and pooled. Plasmids were recovered from the bacteria using the Qiagen EndoFree Plasmid Maxi Kit (Qiagen 12362) per the manufacturer's protocol. 10⁶ HEK-293T cells were plated into each of 75 10-cm tissue culture dishes and allowed to adhere overnight. The following day, each dish was transfected with 2.5 μ g p9.81, 2.5 μ g Brunello CRISPR library, and 1 μ g pMDG along with 18 μ L polyethyleneimine transfection reagent (Sigma 408700). After 72 hours, the culture supernatant was harvested, centrifuged at 3500 rpm for 5 minutes, aliquoted, and stored at -80°C. WI-26 and HBE cells were transduced at an

MOI of 0.3, selected with puromycin, and cultured for two weeks. Cells were then incubated with rEsxA at the LD₉₀ concentration overnight. Surviving cells were harvested and genomic DNA was isolated using the MasterPure Complete DNA & RNA Purification Kit per the manufacturer's protocol. Two rounds of PCR were performed in order to amplify the initial sgRNA and barcode the samples. Amplified products were purified using the AMPure XP-PCR purification kit and sequenced via Illumina HiSeq 2500.

TriCEPS screen

300 µg of either EsxA or transferrin was resuspended in 150 µL 25 mM HEPES pH 8.2. 1.5 µL of the TriCEPS reagent (Dualsystems Biotech) was added to each sample and incubated at 20°C for 90 minutes with gentle agitation. During this time, 6×10^8 Caco-2 cells were detached using 10 mM EDTA in PBS. Cells were split into three aliquots, cooled to 4°C, and pelleted. Each pellet was resuspended in PBS pH 6.5 and sodium metaperiodate was added to a final concentration of 1.5 mM. Cells were then incubated in the dark for 15 minutes at 4°C. Cells were washed twice with PBS pH 6.5 and split into two new aliquots. TriCEPS coupled EsxA was added to one aliquot and TriCEPS coupled transferrin was added to the other aliquot. Samples were then incubated for 90 minutes at 4°C with gentle agitation. Samples were then washed, lysed via sonication, and digested with trypsin. The TriCEPS

reagent:ligand:receptor complex was then affinity purified and peptides were identified using LC-MS analysis.

Immunoprecipitation

EsxA was expressed and purified as described. EsxA or PBS alone was then biotinylated by the Sulfo-SBED reagent according to the manual instructions and excess reagent was removed using size exclusion columns. 1×10^7 HBE or Caco-2 cells were detached using 10 mM EDTA in PBS. Cells were washed, resuspended in HBSS, and incubated with 1.5 μ M EsxA or with PBS alone for 2 hours at 4°C with gentle agitation. Cells were then washed and exposed to UV light for 30 minutes at room temperature to allow for covalent cross-linking. Cells were lysed with RIPA buffer and analyzed by SDS-PAGE followed by either silver staining (Fisher 24612) or Western blotting using an anti-SR-B1 antibody (Abcam 52629).

Adenoid culture and infection

Adenoid samples were obtained from children undergoing adenoidectomies as part of a treatment plan for obstructive sleep apnea. Adenoids were excised and immediately placed in DMEM. Adenoids were dissected into roughly 3-4 pieces, weighed, and mounted in a 2% agar pad such that only the mucosal surface was exposed. The adenoid pieces were then incubated overnight at 37°C in DMEM

supplemented with 20% fetal bovine serum, 2 mM L-glutamine, 1% sodium pyruvate, 1% non-essential amino acids, 1 mM HEPES, 50 ug/mL kanamycin, and 50 ug/mL ampicillin to eliminate the resident bacteria. The following morning, liquid cultures of GFP Mtb grown to mid-log phase were washed three times with PBS, and centrifuged and sonicated to remove clumps. Bacteria were then diluted to 1×10^7 bacteria/mL and 1 mL of inoculum was added to the adenoid and incubated at 37°C for 1 hour. Adenoids were then washed, minced into small pieces, and pushed through a 100 μ m nylon cell strainer (Corning 431752). Cells were centrifuged, washed in ACK lysis buffer, and then resuspended in FACS buffer (PBS + 2% FBS). Cells were stained with a 1:100 dilution of mouse anti-EpCAM Brilliant Violet 421 (Biolegend 324219), mouse PE-NKM-16-2-4 (Milteny 130-102-150), rabbit anti-SR-B1, or normal rabbit IgG in FACS buffer, washed, and then incubated with a 1:500 dilution of AlexaFluor 488 conjugated donkey-anti-rabbit secondary antibody (Thermo R37118). Cells were washed and fixed in 4% paraformaldehyde for one hour followed by counting on an LSRII flow cytometer and analyzed using FlowJo software.

Mouse NALT/human adenoid immunofluorescence

Mouse NALT sections were obtained as previously described. Briefly, mouse NALT and human adenoid specimens were embedded in paraffin, sectioned to 5 μ m slices, and mounted on glass slides. Slides were then deparaffinized using xylene

and ethanol washes followed by heat mediated antigen-retrieval in 10 mM sodium citrate (pH 6.0). Endogenous peroxidase activity was quenched and slides were blocked in 10% donkey serum in PBS for three hours at room temperature. Slides were washed with PBS and incubated with a 1:100 dilution of mouse NKM 16-2-4 and rabbit anti-SR-B1 in 2% donkey serum in PBS overnight at 4°C. Slides were then washed with PBS and incubated with a 1:500 dilution of AlexaFluor 568 conjugated goat-anti-mouse secondary antibody (Thermo A-11004) or with HRP conjugated donkey-anti-rabbit secondary antibody (Thermo A16023) in 2% donkey serum in PBS for 1 hour at room temperature. Slides were then washed with PBS and incubated with Cy5 tyramide (Perkin Elmer SAT705A001EA) for 8 minutes. Slides were then washed with PBS, incubated with DAPI, washed with PBS, mounted in Prolong Gold antifade reagent, and imaged using an AxioImager MN microscope (Zeiss).

CHAPTER THREE

Results

T7SS OF *M. TUBERCULOSIS* IS NECESSARY AND ESXA IS SUFFICIENT TO MEDIATE TRANSLOCATION ACROSS M CELLS

Introduction

One potential explanation for the development of extrapulmonary TB centers upon the mucosa-associated lymphoid tissue (MALT). Specialized epithelial cells known as M cells overlie the MALT and translocate luminal material to basolateral antigen presenting cells [18]. Using scanning electron microscopy, we have previously identified Mtb binding to the surface of M cells in vitro and the resulting formation of pore-like structures on the M cell surface [31]. Based on the morphology of the cells, I hypothesized that Mtb may be forming pores on the surface of M cells to facilitate invasion of the host cell. One of the best characterized pore forming molecules expressed by Mtb is EsxA, a protein that makes up part of the RD1 locus lost in the attenuated BCG strain of Mtb (Fig. 1) [40]. EsxA is secreted as a heterodimer with EsxB and is thought to dissociate from EsxB under acidic conditions [54]. EsxA is secreted using a specialized type VII secretion system (T7SS) through which several effector molecules are secreted through the bacterial channel protein EccD1 [55]. Based on the known pore-forming ability of EsxA [41] and the observation that pores are found on the surface of M cells after incubation with Mtb [31], I hypothesized that EsxA and the T7SS may promote translocation of Mtb through M cells.

Here I identify the Mtb T7SS as necessary for the translocation of Mtb through M cells in vitro and in vivo. EsxA is sufficient to mediate binding and translocation through M cells in vitro, possibly by binding a receptor on the surface of M cells. These novel findings identify Mtb T7SS and EsxA as being bacterial mediators of binding and translocation through M cells.

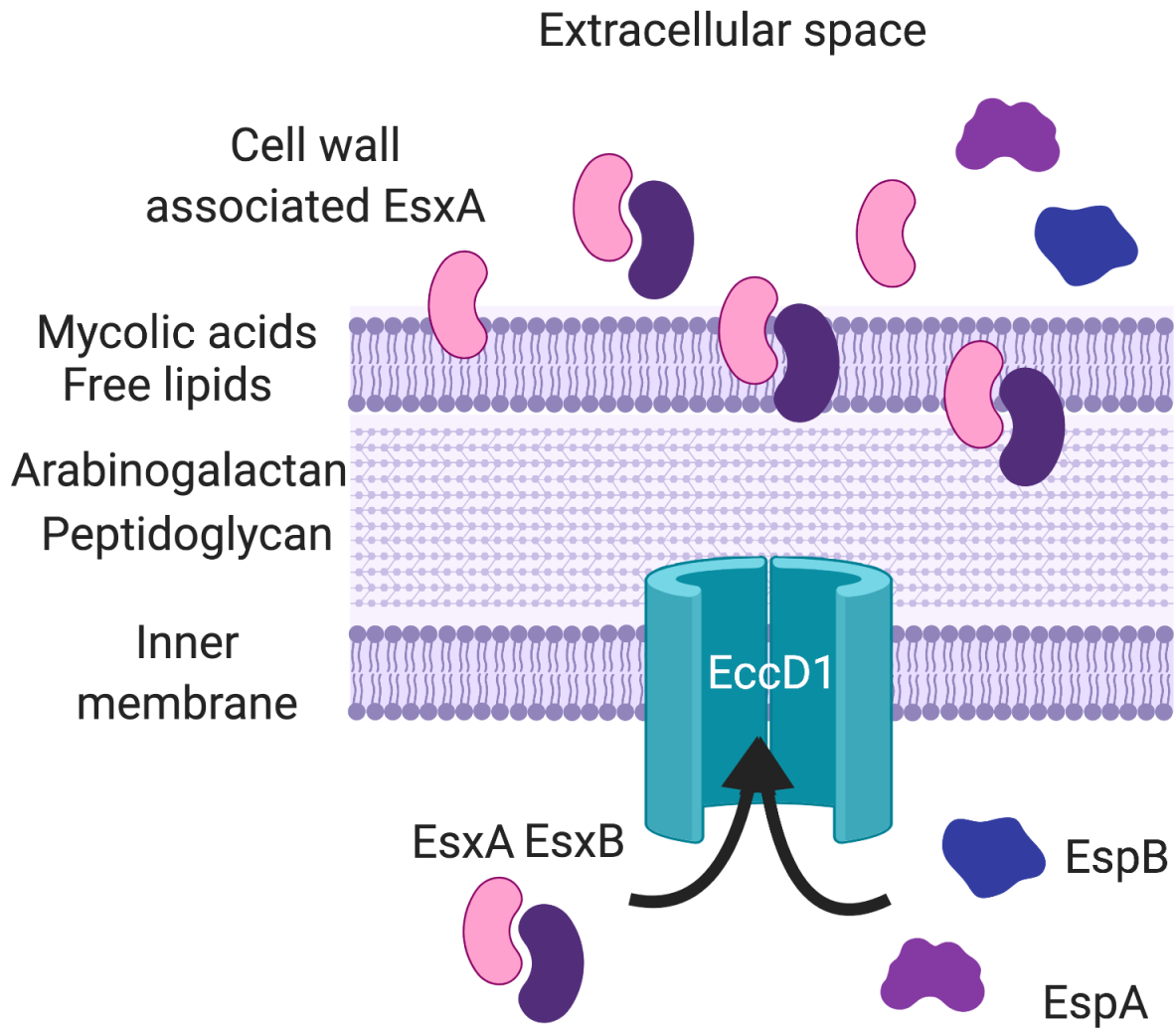


Figure 1. Schematic of Mtb Esx-1 secretion system. Mtb encodes a number of type VII secretion systems including the Esx-1 secretion system through which effector proteins such as EsxA, EsxB, EspA, and EspB are secreted through the bacterial channel EccD1.

Results

In vitro model of M cell development

In order to model the interaction of Mtb with M cells, I utilized an in vitro model of M cell development first described over 20 years ago (Fig. 2) [56]. In this model, epithelial cells are cultured in the apical chamber of transwell inserts containing 3 μm pores. Raji B cells are then added to the basal compartment of transwells (hereafter referred to as “Raji B transwells”), thereby inducing some of the overlying epithelial cells to differentiate into M cells through the interaction of RANKL (either secreted or Raji B cell bound) with RANK on epithelial cells [57]. Alternatively, media alone is added to the basal compartment of transwells (hereafter referred to as “control transwells”), in which case there is little to no M cell differentiation. While this model first utilized Caco-2 cells, a human colonic epithelial cell line, in the apical chamber [56], we have extended this model using 16-HBE cells [31], a human bronchial epithelial cell line that is more physiologically relevant as Mtb is a respiratory pathogen.

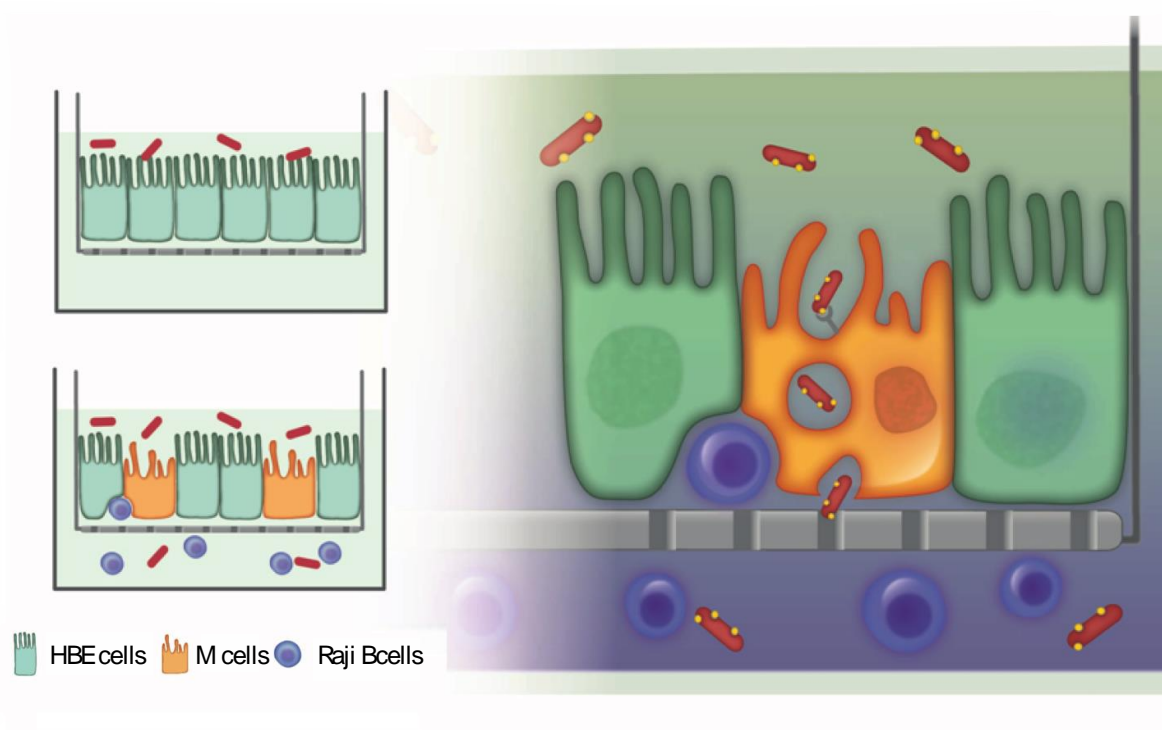


Figure 2. Model of in vitro M cell development. Unlike control transwells that only have epithelial cells present (top left), Raji B transwells utilize the co-culture of epithelial cells and B cells (bottom left) to induce some of the epithelial cells to differentiate into M cells. I hypothesize that a bacterial effector (yellow dots on bacteria) binds to a host receptor on M cells (gray structure on apical surface of M cell) that allows for bacterial translocation.

Mtb T7SS is necessary for translocation across M cells in vitro

To test the role of the T7SS in the ability of Mtb to translocate across M cells in vitro, control or Raji B transwells were infected either with WT Mtb or *MtbΔeccD1*. Translocation to the basal compartment was determined after 60 minutes by enumerating bacterial CFU and comparing to the initial inoculum (Fig. 3A). *eccD1* is a membrane pore required for the secretion of substrates through the T7SS (Fig. 1); strains deficient for *eccD1* are functionally deficient for the T7SS as there is no secretion of substrates [55]. Similar to our previous published results, Mtb significantly translocated across Raji B transwells as compared to control transwells [31]. However, *MtbΔeccD1* was unable to translocate across Raji B transwells, implying that the T7SS is required for translocation across M cells in vitro (Fig. 3A). In order to ensure the observed phenotype was not due to the ability of WT Mtb to disrupt the epithelial monolayer, I measured the transepithelial electrical resistance (TEER) before and after the experiment. I observed that the TEER did not change over the course of the infection (Fig. 3B), verifying the integrity of the epithelial monolayer. Taken together, these data suggest that the T7SS is necessary for Mtb to translocate across M cells in vitro.

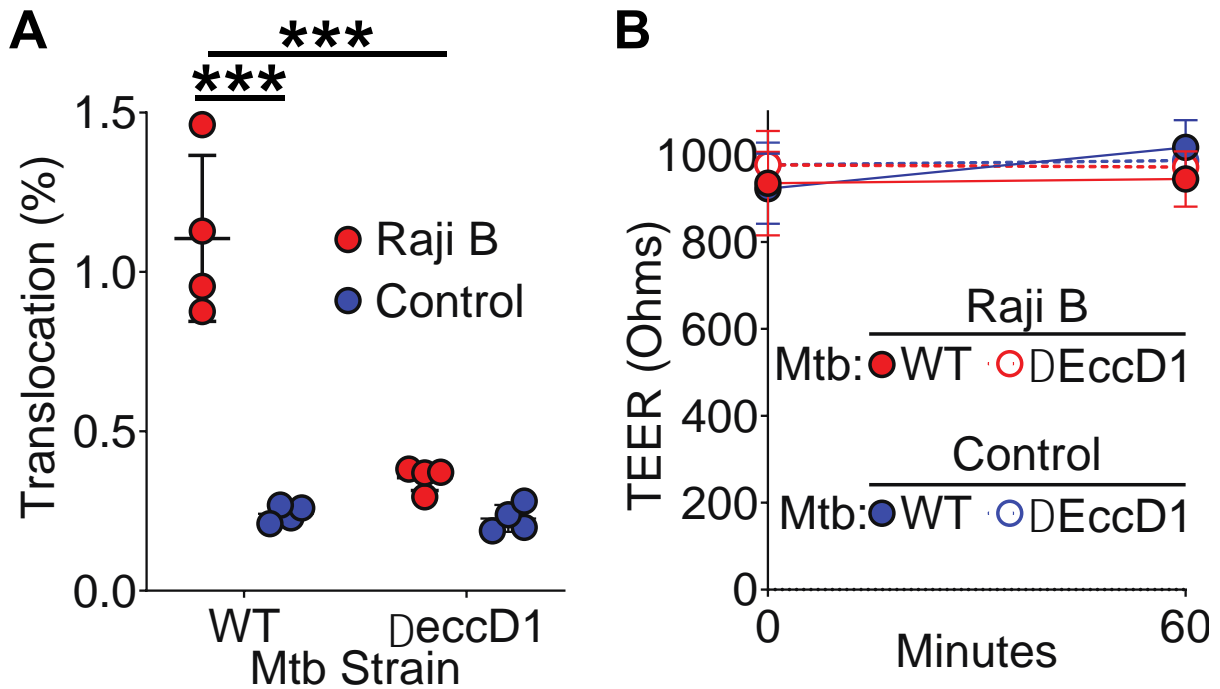


Figure 3. Loss of T7SS reduces ability of Mtb to translocate across M cells in vitro. **A**, WT Mtb or Mtb Δ eccD1 were added to the apical chamber of control or Raji B transwells and percent translocation was determined by comparing the bacterial CFU from the basal compartment after 60 minutes with the inoculum. **B**, TEER measurement of the transwells from **A**. *** $p < 0.001$, Student's t-test

Mtb T7SS is necessary for binding to M cells in vitro

To test if the T7SS of Mtb was required for binding to M cells as well as translocation across M cells, Raji B or control transwells were infected with mCherry Mtb or mCherry Mtb Δ eccD1 at 4°C to prevent endocytosis or translocation of bacteria. Transwells were then washed to remove unbound bacteria, fixed, and analyzed by confocal microscopy (Fig. 4A). To quantify bacterial staining, multiple transwell images were analyzed by ImageJ to determine the area of each field occupied by bacteria (Fig. 4B). I observed Mtb was able to bind to cells on Raji B treated transwells in a T7SS dependent manner, implying that the T7SS was required for bacterial binding and translocation in vitro. I performed a similar experiment where Raji B or control transwells were again infected with mCherry Mtb or mCherry Mtb Δ eccD1 at 4°C. Transwells were washed and lysed to determine the number of bound bacteria by enumerating bacterial CFU (Fig. 4C). I again observed that significantly more Mtb was bound to Raji B treated transwells as compared to control transwells and that this activity depended upon the T7SS. I next attempted to determine if Mtb was binding specifically to M cells upon Raji B treated transwells. I infected Raji B transwells with mCherry Mtb at 4°C, washed away unbound bacteria, and incubated the transwells using the NKM 16-2-4 antibody, an antibody that recognizes the α 1,2-fucose linkage specific to M cells [31, 58]. Unfortunately, the extensive fixation required to safely remove the transwells from the BSL3 facility reduced the binding of the NKM 16-2-4 antibody and I were therefore unable to determine if the majority of Mtb bound cells were NKM positive or negative. Taken

together, these data suggest that the T7SS is required for bacterial binding and translocation across M cells in vitro.

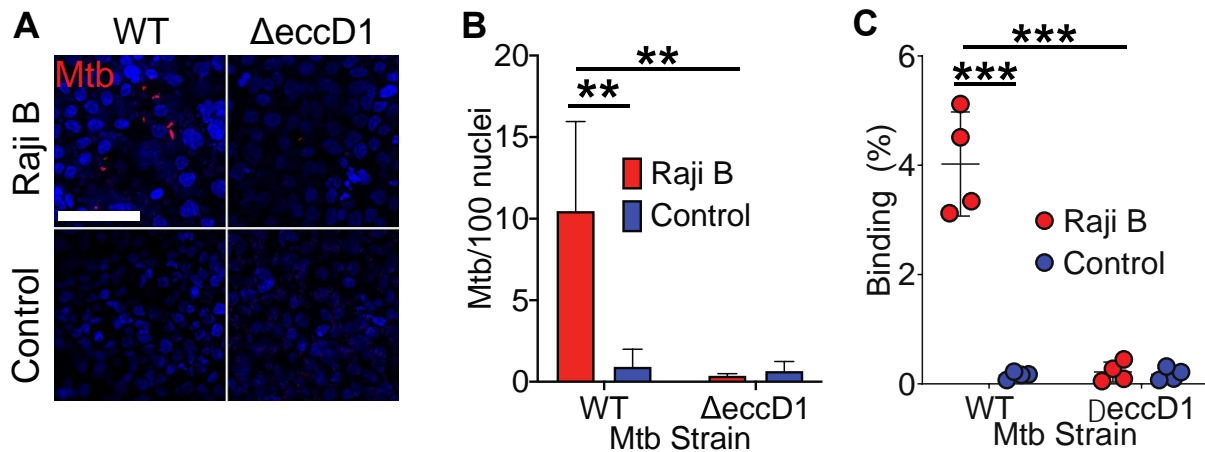


Figure 4. Loss of T7SS reduces ability of Mtb to bind to M cells in vitro. **A**, Raji B or control transwells were incubated with mCherry Mtb or mCherry Mtb Δ eccd1 for 60 minutes at 4°C, fixed, and analyzed by confocal microscopy. Scale bar, 20 μ m. **B**, ImageJ was used to quantify the number of Mtb bound to the surface of transwells from **A**. **C**, Raji B treated or control transwells were incubated with WT or Δ eccd1 Mtb for 60 minutes at 4°C, washed, and then lysed. Percent binding was calculated by comparing bacterial CFU with the initial inoculum. **p<0.01, ***p<0.001 as determined by Student's t test.

EsxA is sufficient to mediate translocation of inert beads across M cells in vitro

I next attempted to determine which substrates secreted through the T7SS may be responsible for the binding and translocation of Mtb across M cells. Two of the most abundant proteins secreted through the T7SS include EsxA and EsxB. To test if either of these proteins were able to interact with M cells, fluorescent beads were conjugated to recombinant EsxA, recombinant EsxB, or to glycine as a control. Beads were then added to the apical chamber of Raji B or control transwells and translocation to the basal compartment was determined after 60 minutes using flow cytometry and compared to the initial inoculum (Fig. 5A). I observed that EsxA conjugated beads were able to translocate across transwells in an M cell dependent manner, implying that EsxA is sufficient to mediate M cell translocation. Translocation of EsxA conjugated beads was not due to any epithelial damage as the TEER remained relatively constant over the course of the infection (Fig. 5B).

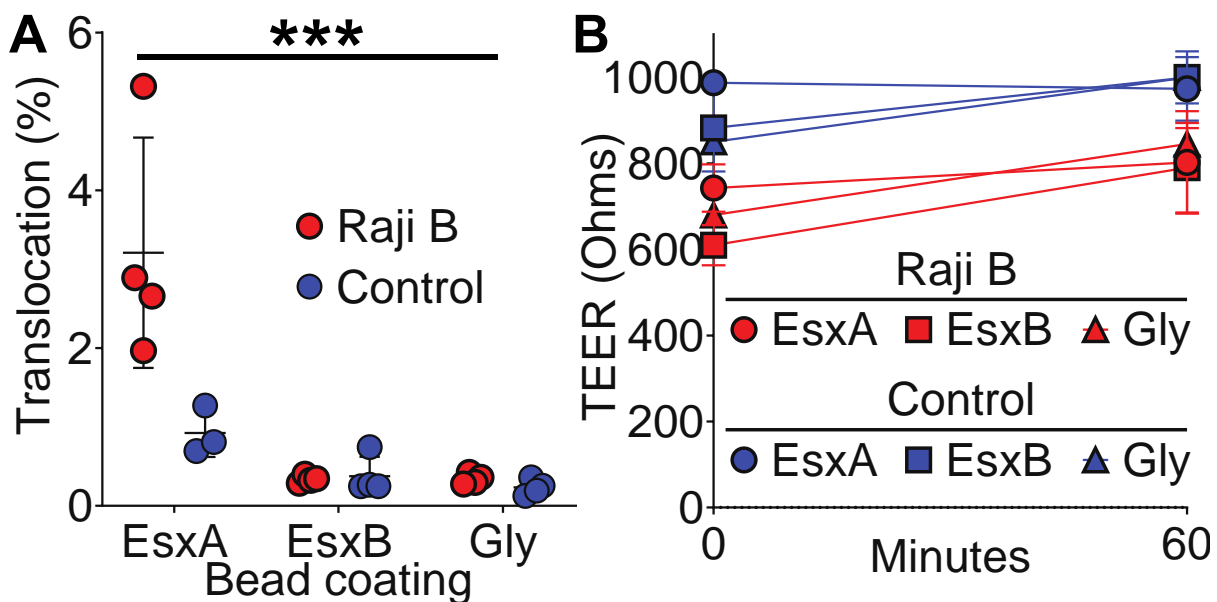


Figure 5. EsxA is sufficient to mediate translocation of inert beads across M cells in vitro. **A**, Fluorescent beads were coated with either EsxA, EsxB, or glycine as a control and added to the apical chamber of control or Raji B treated transwells. Percent translocation was determined by dividing the number of particles in the basolateral compartment after 60 minutes with the initial inoculum. **B**, TEER measurement of the transwells from **A**. *** $p < 0.001$ as determined by Student's t test.

EsxA binds to the surface of M cells in vitro

To determine if the ability of EsxA to mediate translocation across M cells in vitro was due to its ability to bind to the surface of these cells, Raji B or control transwells were incubated with biotinylated recombinant EsxA at 4°C. Transwells were then washed, fixed, incubated with NKM 16-2-4 and Alexa Fluor 488 conjugated streptavidin, and analyzed by confocal microscopy (Fig. 6A). Consistent with the idea that Raji B cells promote M cell differentiation, I observed greater levels of NKM 16-2-4 signal on Raji B transwells as compared to control transwells (Fig. 6A,B). This was not due to a difference in the number of overall cells on the transwells as the number of nuclei present on both groups of transwells was roughly equivalent (Fig. 6A,C). I also observed greater numbers of EsxA positive cells on Raji B treated transwells as compared to control transwells (Fig. 6A,D). Additionally, the majority of EsxA positive cells on Raji B transwells were also positively stained with the NKM 16-2-4 antibody (Fig. 6A,E). Taken together, I believe this data shows that EsxA is sufficient to mediate binding to and translocation across M cells in vitro, potentially by binding a surface receptor.

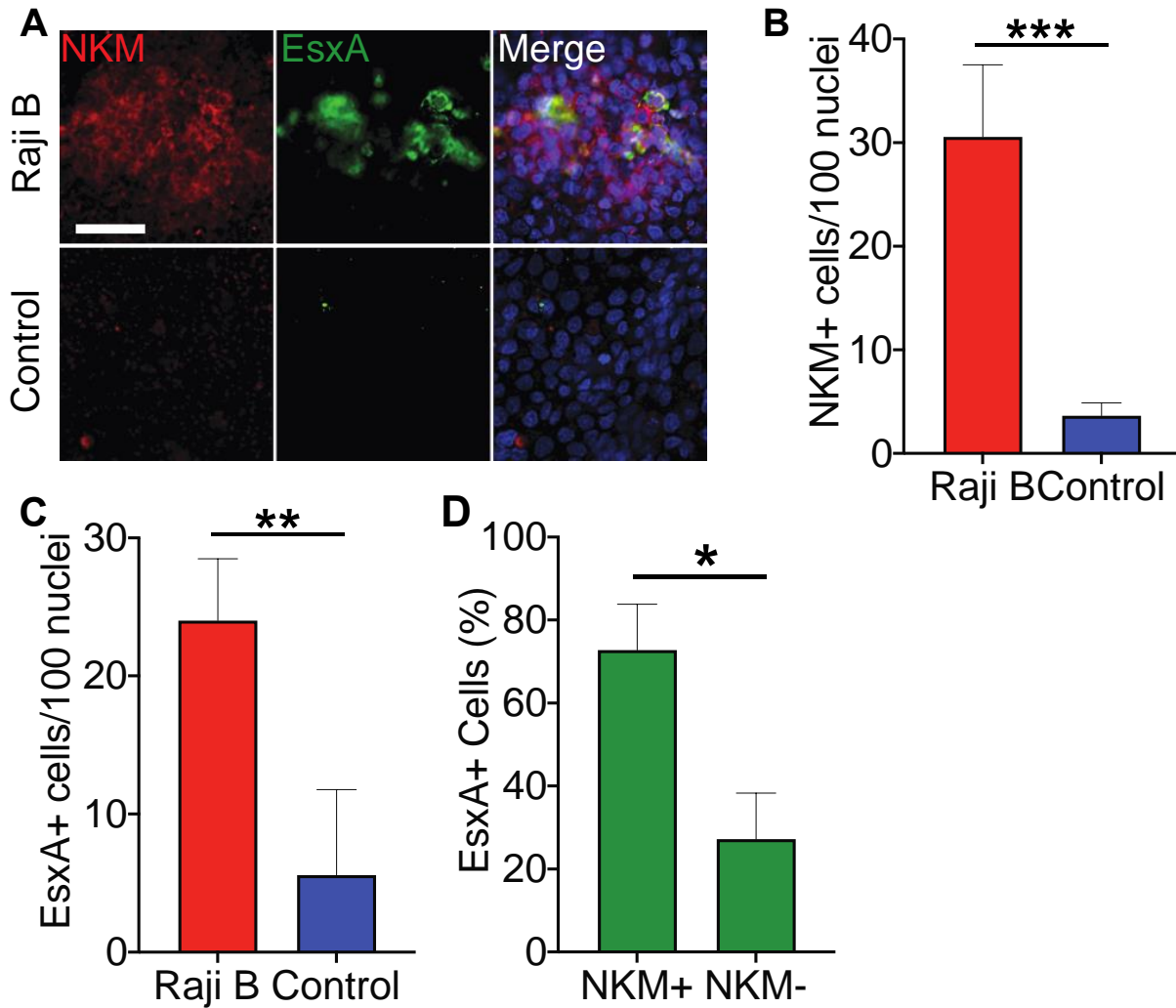


Figure 6. EsxA binds to the surface of M cells in vitro. **A**, Raji B or control transwells were incubated with biotinylated EsxA, fixed, and stained with NKM 16-2-4 (red) and Alexa Fluor 488 conjugated streptavidin (green). Scale bar, 30 μ m. **B,C**, The number of NKM positive cells (**B**) and EsxA positive cells (**C**) from the staining described in **A** was quantified using ImageJ. **D**, The percentage of NKM+ and NKM-

EsxA positive cells from Raji B transwells was quantified using ImageJ. * $p < 0.05$,

** $p < 0.01$, *** $p < 0.001$ as determined by Student's T test.

Expression and purification of recombinant EsxA

Our next goal was to perform a structure-function analysis of EsxA, an assay that required a substantial amount of recombinant protein. To that end, I expressed and purified an N-terminally 6xHis tagged EsxA from inclusion bodies within *E. coli* [48]. EsxA was then denatured with 8 M urea and re-folded in the presence of the zwitterionic detergent ASB-14. The detergent was then dialyzed away to yield rEsxA (Fig. 7). As a control, EsxB was purified alongside EsxA following the same protocol.

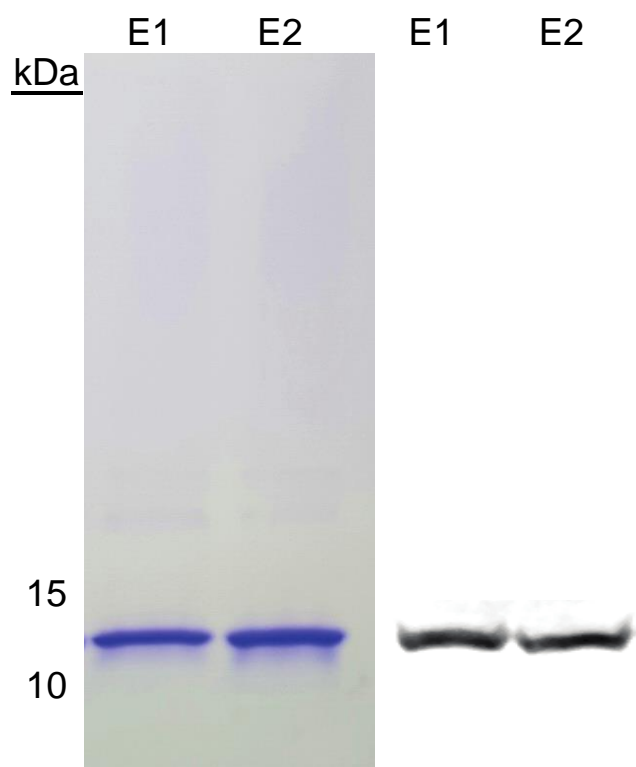


Figure 7. Expression and purification of recombinant EsxA. Coomassie (left) and western blot (right) using an EsxA specific antibody of pooled elution fractions from two independent protein purification experiments (E1 and E2).

Recombinant EsxA demonstrates hemolytic, cytolytic, and binding activities

I first verified that the rEsxA I purified exhibited the published activities attributed to EsxA, such as the ability of EsxA to lyse both red blood cells (RBCs) and WI-26 cells, a human type II pneumocyte cell line [41]. I compared the lytic activities of EsxA obtained from BEI Resources (hereafter referred to as “BEI EsxA”), an ATCC subsidiary that supplies Mtb researchers with purified proteins/lipids/etc., with the EsxA and EsxB I produced (hereafter referred to as “rEsxA” and “rEsxB”). Specifically, sheep RBCs and WI-26 cells were incubated with increasing concentrations of protein. RBC lysis was determined by measuring the amount of hemoglobin released into the supernatant. WI-26 cell lysis was determined by measuring the amount of lactate dehydrogenase, a glycolytic enzyme normally found within the cell, released into the culture supernatant. For both RBC and WI-26 lysis, both BEI EsxA and rEsxA were able to mediate lysis with similar efficiency (Fig. 8A,B). Importantly, rEsxB was unable to cause lysis, implying that ASB-14 was successfully removed during the purification process. To test the ability of rEsxA to bind to epithelial cells, I performed a modified ELISA assay where HBE cells were plated in a 96 well plate and incubated with increasing amounts of protein. Bound protein was detected using HRP-conjugated antibodies targeting the 6xHis tag. I observed that both BEI EsxA and rEsxA were able to bind to HBE cells with similar efficiency while rEsxB was unable to bind to these cells (Fig. 8C). Taken together, these data suggest that rEsxA successfully recapitulates the published activities as well as BEI EsxA and that both EsxA products bind HBE cells.

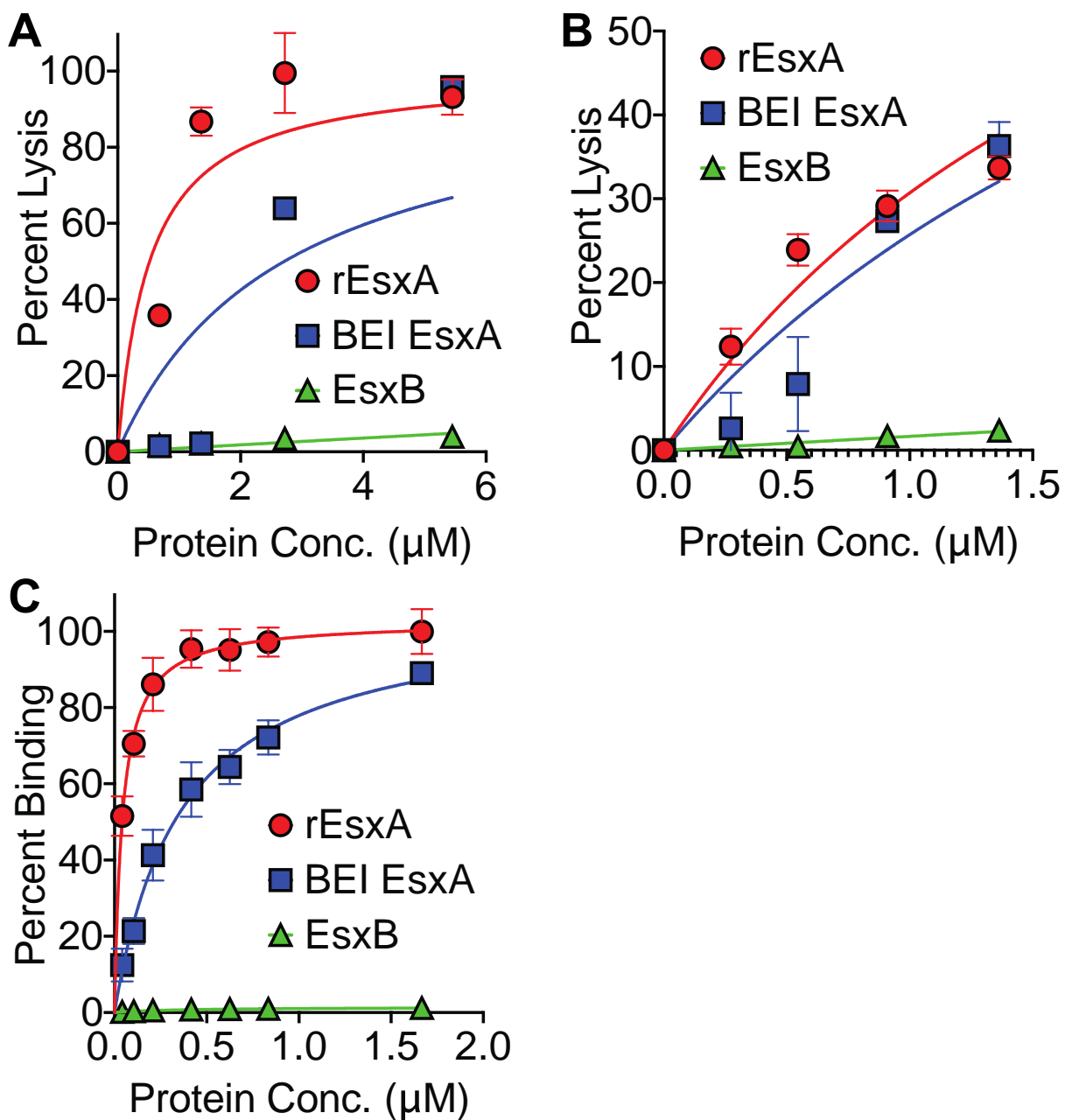


Figure 8. Recombinant EsxA demonstrates hemolytic, cytolytic, and binding activities. A, Red blood cells were incubated with recombinant protein. Lysis was determined by measuring the amount of hemoglobin released into the supernatant

by measuring Abs₄₀₅. **B**, WI-26 cells were incubated with recombinant protein. Lysis was determined by measuring release of lactate dehydrogenase into the supernatant. **C**, HBE cells were incubated with recombinant protein. Bound protein was detected using HRP-conjugated antibodies and ELISA substrate.

EsxA S48A has reduced hemolytic, cytolytic, and binding activities

As mentioned previously, EsxA interacts with both laminin on pneumocytes [41] and with beta-2-microglobulin on macrophages [42]. EsxA is also a pore-forming molecule able to cause hemolysis and cytolysis, potentially through direct membrane insertion [41, 43]. I hypothesized that specific amino acids in EsxA could mediate these two disparate processes (namely binding and lysis) and that it may be possible to separate binding of EsxA to its putative receptor on M cells from its other known activities. Identification of these residues would allow me to complement *Mtb*Δ*esxA* with EsxA mutants that were capable of mediating either binding or lysis and allow for the dissection of these two roles of EsxA in vivo. To identify these residues, I performed a multiple sequence alignment of the EsxA protein sequence from *Mtb* and closely related species and identified conserved residues that were predicted to be exposed on the protein surface (Fig. 9A). I next commercially synthesized DNA sequences encoding for encoding for point mutants of EsxA where the conserved residue was substituted for alanine. EsxA mutants were then expressed and purified from *E. coli* as described before. Of the 12 mutants originally chosen, 3 mutants were successfully cloned, expressed, and purified (Fig. 9B). When assayed via binding, cytolytic, and hemolytic activities, EsxA S48A (hereafter referred to as “M8”) showed reduced activity in all three assays (Fig. 9C,D,E).

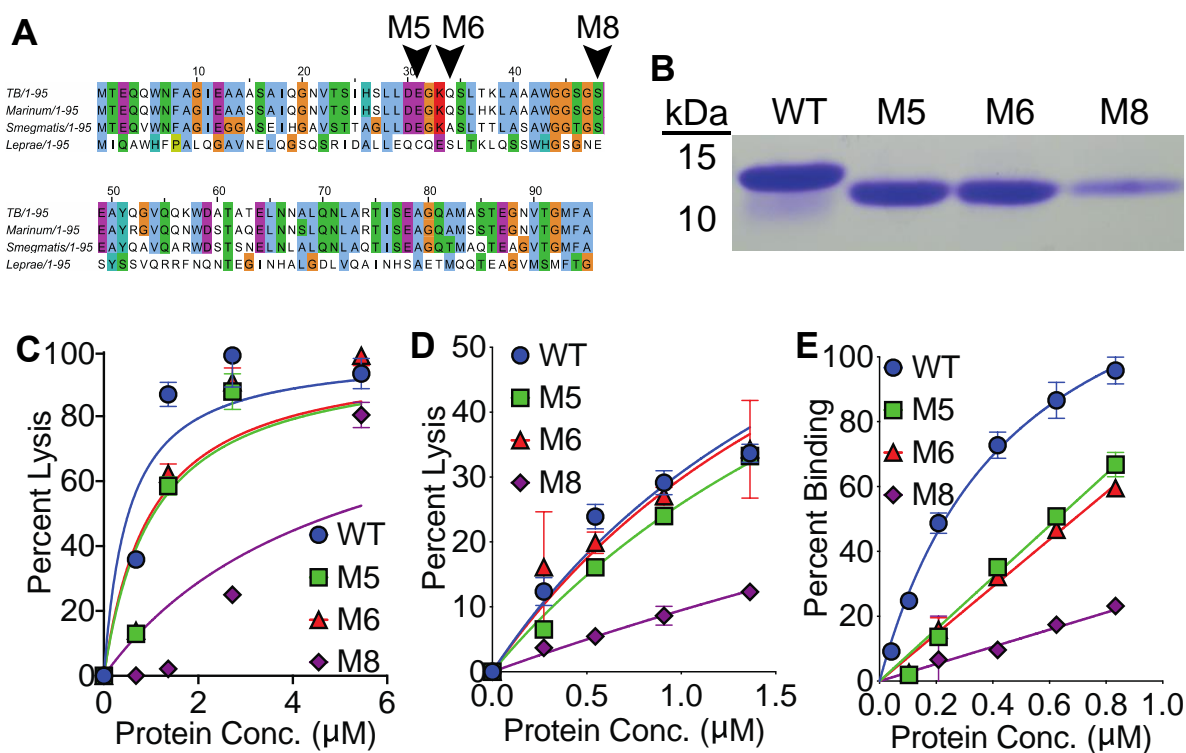


Figure 9. EsxA S48A shows a reduced hemolytic, cytolytic, and binding activity. **A**, EsxA from Mtb was aligned against closely related homologues to identify conserved residues. Black arrows denote mutated amino acids. **B**, Coomassie comparing WT EsxA and three point mutants. **C,D,E**, WT EsxA and mutants were assayed for hemolytic activity (**C**), cytolytic activity (**D**), and binding activity (**E**).

ASB-14 contamination may explain EsxA mediated hemolysis, cytolysis, and binding

Although the protocol I used to purify and refold EsxA has been widely used by many groups over many years [48], I grew concerned about possible ASB-14 contamination of the final protein preparation and hypothesized that some activities attributed to EsxA could be due to detergent contamination. In order to determine the approximate concentration of ASB-14 in the final protein preparation, I performed a dichloromethane/methanol extraction of EsxA obtained from BEI, EsxA I produced, and ASB-14 standards all resuspended in PBS. I isolated the detergent-containing organic layer and determined the amount of detergent present within the fraction by comparing the signal from the protein preparations against the known standards using mass spectrometry (Fig. 10A). I estimated that both my EsxA preparation and the BEI EsxA preparation were contaminated with ASB-14 at an approximate concentration of 4 μ M. Even at a 1:100 dilution (the maximal dilution of the EsxA stocks used in cytolysis or hemolysis assays) of 4 μ M ASB-14, I observed both hemolysis and cytolysis at levels equivalent to a 1:100 dilution of rEsxA (Fig. 10B,C). I performed additional control experiments and determined that rEsxA was binding non-specifically to the plates used in the modified ELISA assay (Fig. 10D). Taken together, this data shows that the established hemolytic and cytolytic activities reported for EsxA as well as the binding activity I observed in my modified ELISA assay may be in part due to detergent contamination and must be carefully re-evaluated.

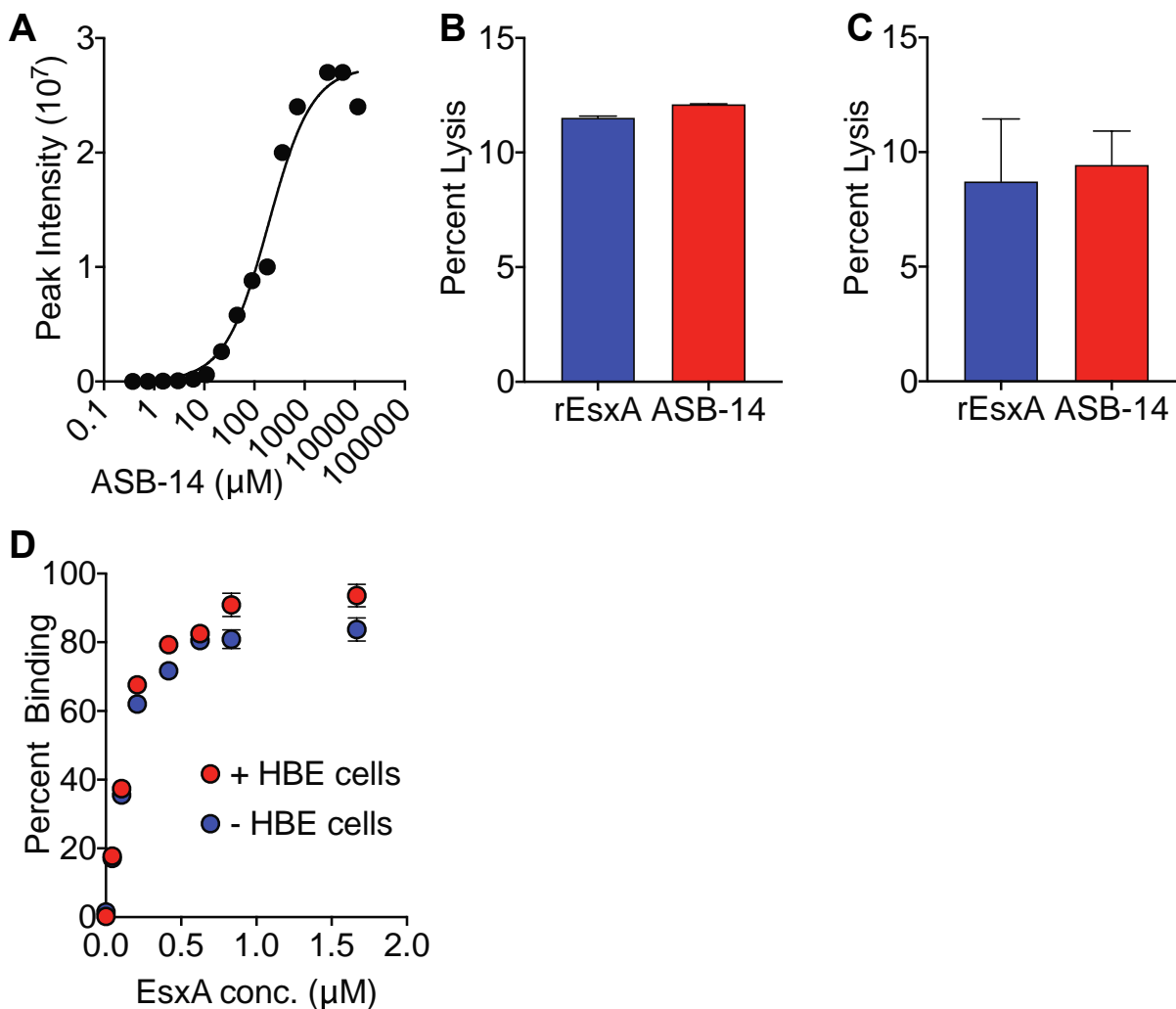


Figure 10. EsxA hemolytic, cytolytic, and binding activities may be due to ASB-14. **A**, Peak intensity of known concentrations of ASB-14 was used to generate a standard curve to estimate ASB-14 contamination of rEsxA at 4 μM . **B,C**, Hemolysis (**B**) or cytolysis assay (**C**) were performed using a 1:100 dilution of rEsxA or a 1:100 dilution of 4 μM ASB-14. **D**, Binding assay for rEsxA was performed using plates with or without HBE cells present.

Mtb T7SS is necessary for translocation across M cells in vivo

I next determined the role of the T7SS of *Mtb* in bacterial translocation across M cells in vivo. To answer this question, BALB/c mice were intranasally infected with either WT *Mtb*, *Mtb* Δ *eccD1* (Fig. 11A), or *Mtb* Δ *esxA* (Fig. 11B) to limit the infection to the upper airways, including the NALT. Loss of *EsxA* disrupts the proper assembly of the protein complex required for effector secretion through the T7SS. This therefore leads to a second T7SS deficient strain of *Mtb* as no effectors can be secreted through this pathway [55]. Mice were either sacrificed on day 0 and the initial inoculum of bacteria deposited within the NALT was determined by plating for bacterial CFU or sacrificed on day 7 to determine translocation of bacteria to the cervical lymph nodes, the draining lymph nodes of the NALT. While there was no difference in the initial inoculum between the three strains, I observed significantly more bacteria recovered from the cervical lymph nodes of the mice infected with WT *Mtb* as compared to the *Mtb* Δ *esxA* or *Mtb* Δ *eccD1* strains, implying that the T7SS is required for translocation in vitro and in vivo.

An alternative explanation for this observation is that the reduced number of bacteria recovered from the cervical lymph nodes on day 7 is not due to a translocation defect but rather due to a defect in the ability of the T7SS deficient strains to survive within the host. In order to address this, mice were infected either with WT *Mtb* or *Mtb**cor::Tn7* (Fig. 11C), a transposon mutant of *Mtb* that is deficient for *cor*, a carbon monoxide resistance gene. Previous work has shown that *Mtb**cor::Tn7* is attenuated in vivo in mice [59]. Again, mice were sacrificed on day 0 to determine the initial

inoculum deposited within the NALT by enumerating bacterial CFU or sacrificed on day 7 to determine translocation of bacteria to the cervical lymph nodes. Unlike the T7SS deficient strains of Mtb, the number of bacteria recovered from the cervical lymph nodes of mice infected with WT Mtb was similar to that of mice infected with *Mtbcor::Tn7*. This implies that the reduced number of bacteria recovered from lymph nodes of mice infected with the T7SS deficient strains was not solely due to an attenuation defect. Taken together, I believe this data shows that the T7SS is required for bacterial translocation across M cells in vivo.

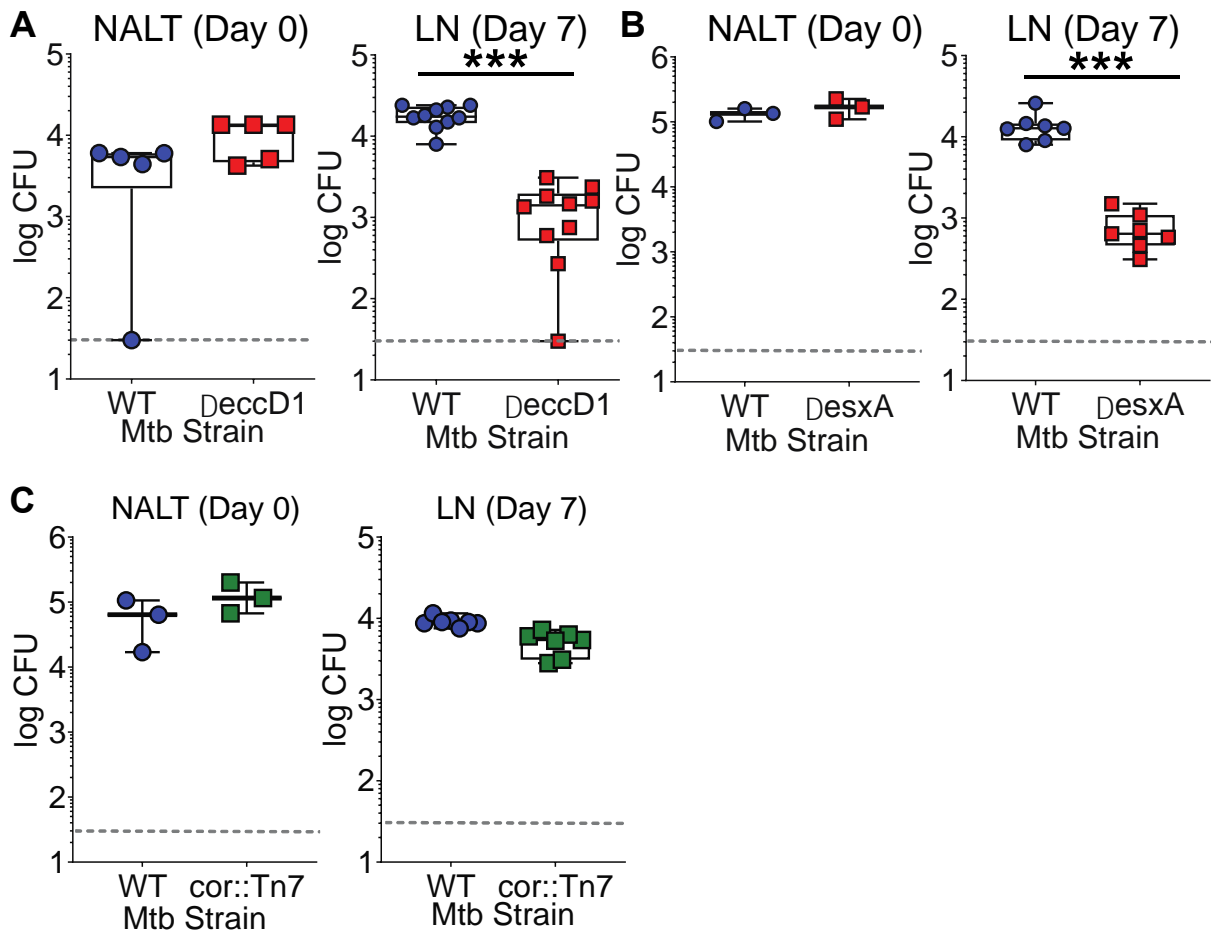


Figure 11. Loss of T7SS reduces translocation of Mtb across M cells in vivo.

A,B,C, Mice were infected either with WT Mtb, Mtb Δ eccD1(**A**), Mtb Δ EsxA(**B**), or Mtb $cor::Tn7$ (**C**) via an intranasal infection and CFU was determined in the NALT on day 0 (left) (n=3-5/group) or in the cervical lymph nodes on day 7 (right) (n=7-10/group). ***p<0.001 compared to WT by Mann-Whitney test.

Discussion

Here I identify the Mtb T7SS as being necessary and EsxA as being sufficient to mediate bacterial translocation through M cells in vitro. Using mouse models of infection, I demonstrate that the T7SS is also required for bacterial translocation in vivo. While attempting to dissect the known lytic properties of EsxA from its proposed function in binding M cells, I determine that ASB-14 contamination may explain the proposed pore-forming ability of recombinant EsxA. The reduced ability of EsxA S48A to mediate cytolysis, hemolysis, and binding as compared to the wild-type protein may reflect a reduced ability to bind ASB-14 and therefore a lower concentration of contaminating detergent in the final protein preparation, although this remains to be tested.

This study adds to the growing body of literature questioning the pore-forming activity of recombinant EsxA. For example, recombinant EsxA purified in the presence of ASB-14 retains its lytic properties even after digestion by proteinase K [47], implying that residual detergent and not protein may be responsible for red blood cell lysis. Additionally, a comparison of published reports of recombinant EsxA being purified in the presence or absence of ASB-14 demonstrated that studies highlighting the lytic properties of EsxA were always performed with ASB-14 treated EsxA [47]. Due to the small size of the protein and the fact that adding a tag may interfere with appropriate secretion of the protein under native conditions [60], it is difficult to determine what activities Mtb EsxA may have. Because of its pivotal role

in promoting Mtb virulence, it is critical to re-examine the function of EsxA in an unbiased fashion in the hopes of better understanding Mtb infection.

CHAPTER FOUR

Results

IDENTIFICATION OF SR-B1 AS AN ESXA RECEPTOR REQUIRED FOR MTB BINDING AND TRANSLOCATION

Introduction

A number of receptors utilized by macrophages for the uptake of Mtb have been described [33, 34]. Additionally, EsxA itself binds beta-2 microglobulin to impede antigen presentation [42] and laminin to aid in Mtb escape [41]. My previous work demonstrated the interaction of Mtb and EsxA with M cells in vitro. Previous work characterizing the interaction between bacteria and M cells has demonstrated that host receptors are often required for bacterial binding and uptake. For example, FimH, expressed by commensal and pathogenic bacteria binds to GP2 on the surface of host M cells to facilitate bacterial binding and translocation. Based on this model, I therefore hypothesize that M cells express a receptor that allows for the binding and translocation of Mtb.

In order to identify the EsxA receptor, I performed a modified co-immunoprecipitation assay utilizing the TriCEPS reagent, a molecule able to covalently cross-link a ligand to its potential receptor and thereby stabilize transient interactions [61]. The TriCEPS reagent is comprised of three functional groups: an N-hydroxysuccinimidyl ester group that allows for covalent bond formation between the reagent and amine

groups, such as those found on the N-terminus of proteins and on lysine side chains; a hydrazine covalent reaction site that allows for covalent bond formation between the reagent and aldehyde groups formed on glycoproteins following a gentle oxidation step; and a biotin group that allows for affinity purification of the ligand:TriCEPS:receptor complex and subsequent mass spectrometric analysis to identify potential receptors. By using a cross-linking molecule such as TriCEPS, the interaction between ligand and receptor is maintained even under the harsh denaturing conditions, high temperatures, or high detergent concentrations required for cell lysis.

Utilizing the TriCEPS assay, I identified scavenger receptor class B type I (SR-B1) as an interaction partner for EsxA. SR-B1 is a high-density lipoprotein receptor that mediates cholesterol uptake and has therefore been primarily studied in endothelial or hepatic cells the context of lipid transport, atherosclerosis, and cardiac function [62]. However, within the respiratory system, SR-B1 in conjunction with LOX-1, another scavenger receptor family member, is required for the sensing of dsRNA by human airway epithelial cells [63]. SR-B1 is also expressed on alveolar macrophages, although SR-B1 deficient macrophages are still able to uptake Mtb [36]. However, blockade of SR-B1 and MARCO, another scavenger receptor family member, decreases uptake of Mtb by mesenchymal stem cells [37]. These studies highlight how SR-B1 may be dispensable in some systems for Mtb uptake but required in others.

Here I show that SR-B1 is an M cell specific receptor in vitro and that loss of SR-B1 reduces EsxA binding and Mtb binding and translocation through M cells in vitro. These findings identify SR-B1 as the first M cell receptor required for translocation of a major airway pathogen.

Results

Survival based CRISPR screen did not identify an EsxA receptor

Prior to performing the control experiments demonstrating that ASB-14 contamination was in part leading to EsxA mediated cytolysis, I hypothesized that binding preceded lysis in EsxA mediated cell death. I therefore hypothesized that cells lacking the receptor or any pathway component downstream of the receptor that signals a cell death pathway would be protected from EsxA mediated cytolysis. In order to identify the EsxA receptor, I performed a whole-genome CRISPR (clustered regularly interspaced short palindromic regions) screen utilizing the Brunello human CRISPR knockout pooled library, a library containing 4 sgRNAs targeting every gene in the human genome [64]. Each sgRNA was encoded by an individual plasmid that also encoded for expression of the Cas9 protein as well as for puromycin resistance. Lentivirus encoding for the Brunello library were created and HBE cells and WI-26 cells were transduced at an MOI of approximately 0.3 to minimize the number of cells transduced with multiple sgRNAs. Approximately 1.5 x

10^8 cells were transduced to yield an approximately 500x coverage where each sgRNA was present 500 times in the selected population of cells. Following puromycin selection, surviving cells were maintained for two weeks to allow for Cas9 mediated genetic manipulation. Cells were then incubated either with EsxA at a concentration resulting in 90% cell death or PBS for 24 hours. Surviving cells were harvested and genomic DNA was isolated. Two rounds of PCR were performed to amplify the sgRNAs and barcode the samples prior to being sequenced by an Illumina HiSeq 2500. Although the representation of the sgRNAs prior to treatment with EsxA was robust and the quality of the resulting amplified sgRNAs was high, no sgRNAs were statistically over- or under-represented in the cells treated with EsxA as compared to cells treated with PBS, implying that EsxA mediated cell death is a non-specific process and may be due to residual detergent contamination within the final protein preparation.

TriCEPS screen identifies SR-B1 and ApoE as potential EsxA receptors

In order to identify the EsxA receptor expressed on M cells, I performed a modified co-immunoprecipitation experiment with the DualSystems Biotech group who have developed the TriCEPS reagent, so named for its three functional groups [61] (Fig. 12A). Caco-2 cells were chosen for this experiment as they have been extensively used as a model for M cell development and Caco2/Raji B transwells mirror the trends seen in HBE/Raji B transwells (namely the Mtb T7SS is necessary for translocation and EsxA is sufficient to mediate translocation) (Fig. 12B,C). In the first

step of the process, EsxA is covalently linked to the TriCEPS reagent through the cross-linking of amine groups on EsxA with a *N*-hydroxysuccinimidyl ester site on the TriCEPS reagent. Caco-2 cells were gently oxidized to convert sugar residues on the cell surface to reactive aldehyde groups. TriCEPS:EsxA was then added to the Caco-2 cells, allowing EsxA to bind to its putative receptor. This brought the hydrazine covalent reaction site of TriCEPS in close proximity to the aldehyde groups on the receptor, allowing for a second covalent bond formation. Caco-2 cells were then lysed and the TriCEPS:EsxA:receptor complex was affinity purified using the biotin group present on the TriCEPS reagent and analyzed by LC-MS to identify enriched peptides. As a positive control, this workflow was also performed using the transferrin protein as successful completion of the experiment should detect the interaction of transferrin and the transferrin receptor.

When Caco-2 cells were treated with transferrin, I was able to detect enrichment of both transferrin (TRFE) and the transferrin receptor (TFR1) (Fig. 12D, blue), validating the ability of the screen to detect ligand:receptor interactions. When cells were treated with EsxA, I detected enrichment of EsxA, apolipoprotein E (ApoE), and scavenger receptor class B type 1 (SR-B1) (Fig. 12D, red). I decided to focus on SR-B1 as an EsxA receptor as it is a membrane bound protein that has been previously shown to interact with mycobacterial species, including both *Mtb* [36] and *Mycobacterium fortuitum* [65].

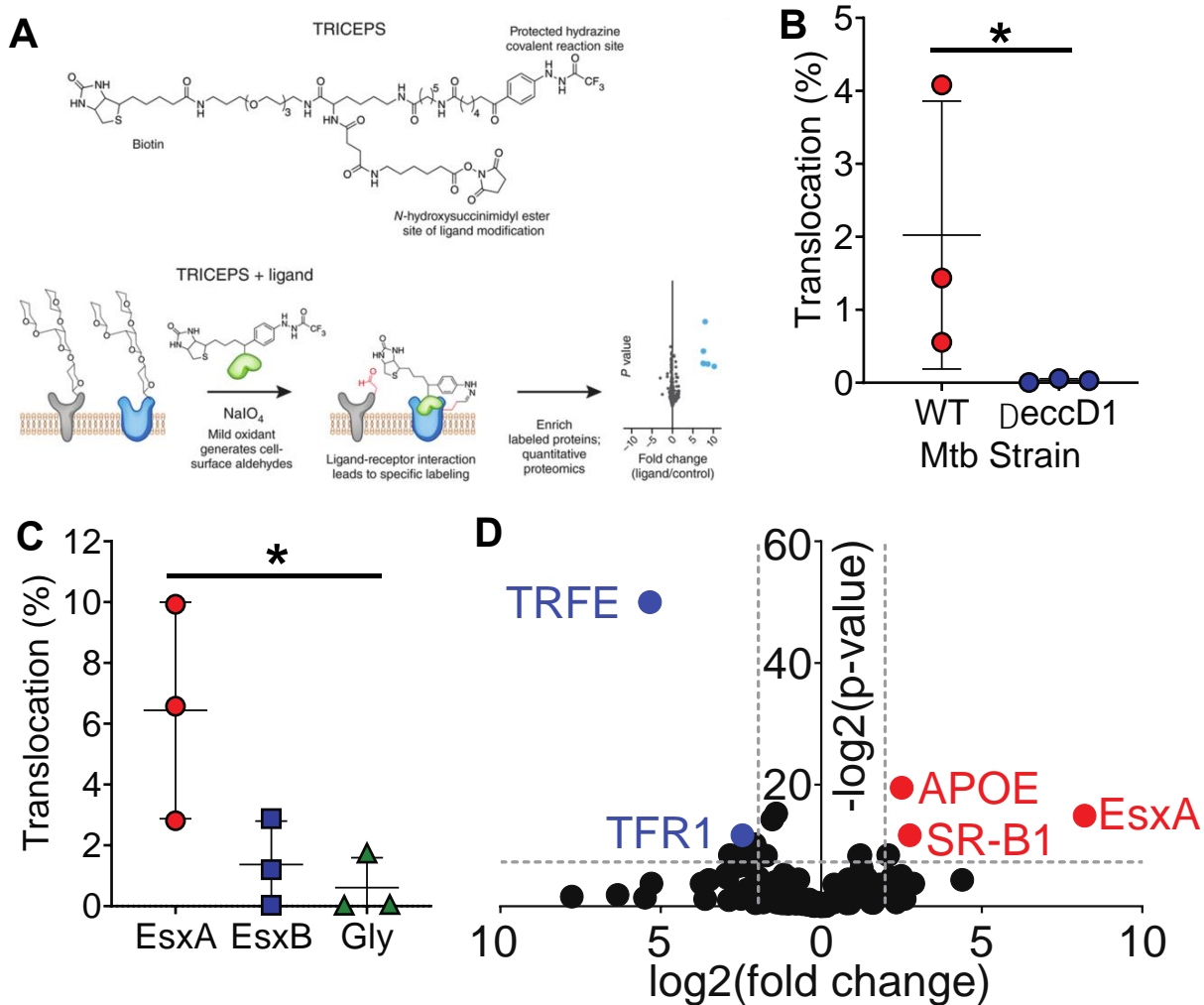


Figure 12. TriCEPS screen identifies SR-B1 and ApoE as potential EsxA receptors. **A**, Schematic of TriCEPS reagent (top) or workflow for receptor identification (bottom). **B**, WT Mtb or Mtb Δ eccD1 were added to the apical chamber of Caco-2/Raji B transwells and percent translocation was determined by comparing the bacterial CFU from the basal compartment after 60 minutes with the inoculum.

C, Fluorescent beads were coated with either EsxA, EsxB, or glycine as a control and added to the apical chamber of Caco-2/Raji B treated transwells. Percent translocation was determined by dividing the number of particles in the basolateral compartment after 60 minutes with the initial inoculum. **D**, Caco-2 cells were treated either with transferrin or EsxA. Transferrin or EsxA was then affinity purified and interacting peptides were determined by mass spectrometry. A volcano plot was generated showing peptides enriched for when cells were treated with transferrin (blue dots on left) or EsxA (red dots on right). TRFE, transferrin; TFR1, transferrin receptor; APOE, apolipoprotein E; SR-B1, scavenger receptor class B type I

EsxA interacts with SR-B1 on both HBE and Caco-2 cells

Based off the results of the TriCEPS assay, I validated the interaction of EsxA and SR-B1 using HBE cells. EsxA was conjugated to Sulfo-SBED biotin label transfer reagent, a cross-linking molecule with a photoactivatable cross-linking group and a cleavable disulfide spacer arm. HBE or Caco-2 cells were removed from tissue culture flasks using EDTA and PBS and incubated with EsxA:Sulfo-SBED or PBS for two hours at 4°C. Cells were washed and exposed to UV light at 365 nm for 30 minutes to allow for crosslinking of Sulfo-SBED with the EsxA receptor. Cells were lysed and incubated with DTT to cleave the cross-linker such that the biotin tag was transferred to the receptor. Biotinylated proteins were affinity purified using streptavidin beads and analyzed by silver stain and western blot. Using HBE cells, I identified a band at approximately 55 kDa that was recognized by an anti-SR-B1 antibody through western blotting (Fig. 13A). Western blotting also recognized a larger species of SR-B1 at approximately 130 kDa (Fig. 13A). Using Caco-2 cells, I again was able to identify the 55 kDa SR-B1 band (Fig. 13B). Taken together, these data suggest that EsxA interacts with SR-B1 on the surface of two epithelial cell lines in vitro.

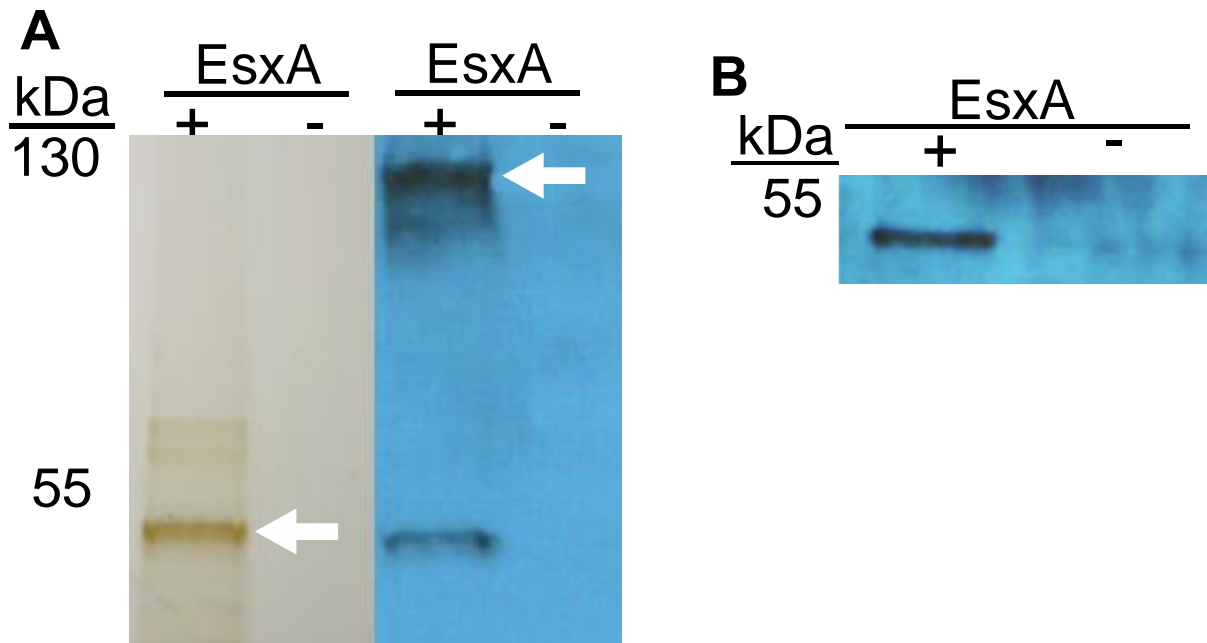


Figure 13. EsxA interacts with SR-B1 on both HBE and Caco-2 cells. A,B, HBE cells (A) or Caco-2 cells (B) were incubated with or without EsxA. EsxA was then affinity purified and interacting peptides were analyzed by SDS-PAGE and silver stain or by Western blot using an anti-SR-B1 antibody.

SR-B1 is preferentially expressed by M cells in vitro

I next analyzed the expression pattern of SR-B1 on M cells as compared to other epithelial cells. To test this, Raji B or control transwells were incubated with biotinylated EsxA, washed, incubated with Alexa Fluor 488 conjugated streptavidin, NKM 16-2-4, and anti-SR-B1 antibodies, and analyzed by confocal microscopy (Fig. 14A). I observed greater expression of SR-B1 on Raji B transwells as compared to control transwells (Fig. 14A,B). Additionally, the majority of SR-B1 positive cells on Raji B transwells were also NKM+ (Fig. 14A,C). Taken together, these data suggest that SR-B1 is a receptor upregulated on M cells in vitro.

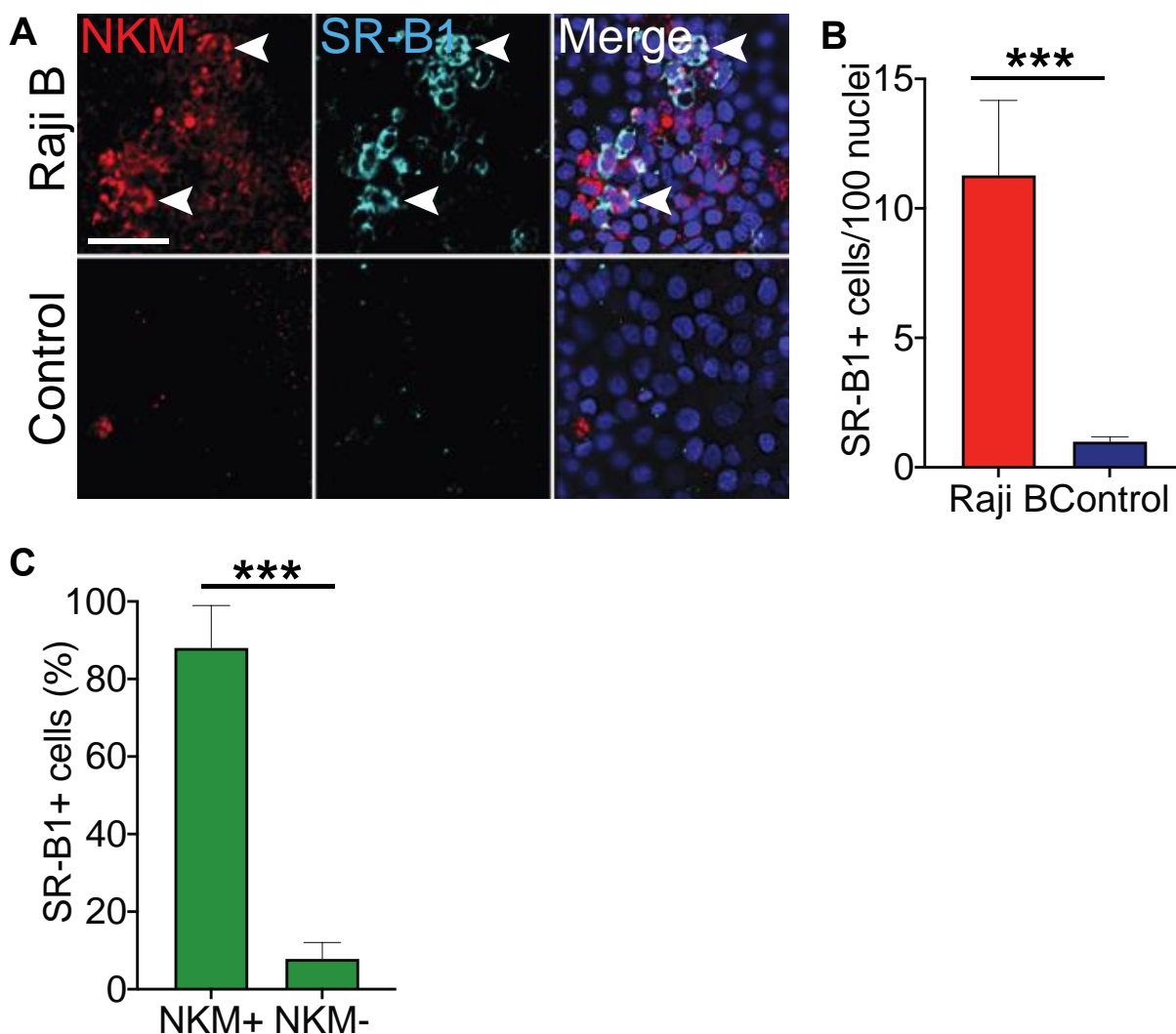


Figure 14. SR-B1 is preferentially expressed by M cells in vitro. **A**, Raji B or control transwells were fixed, stained with NKM 16-2-4 and an anti-SR-B1 antibody, and analyzed by confocal microscopy. Arrows denote examples of double positive cells. Scale bar, 40 μ m. **B**, The number of SR-B1 positive cells from the staining described in **A** was quantified using ImageJ. **C**, The percentage of NKM+ and NKM- SR-B1 positive cells from Raji B transwells was quantified using ImageJ. *** $p < 0.001$ as determined by Student's T test.

Loss of SR-B1 reduces EsxA binding to M cells in vitro

I next examined what functional role SR-B1 had in the ability for EsxA to bind to M cells in vitro. Lentiviral particles containing SR-B1 targeting shRNAs or non-targeting shRNAs were generated and HBE cells were transduced and selected. I observed a robust knock-down of SR-B1 by the SR-B1 shRNA as compared to the non-targeting shRNA (Fig. 15A). shRNA expressing HBE cells were co-cultured with Raji B cells to induce M cell differentiation. Transwells were incubated with rEsxA, fixed, and incubated with NKM 16-2-4, Alexa Fluor 488 conjugated streptavidin, and anti-SR-B1 antibodies prior to being analyzed by confocal microscopy (Fig. 15B). I observed roughly equivalent numbers of nuclei (Fig. 15B,C) and NKM 16-2-4+ cells (Fig. 15B,D) from both groups of transwells, implying that loss of SR-B1 does not negatively impact M cell differentiation. I detected fewer SR-B1+ cells on transwells with SR-B1 shRNA expressing HBE cells (Fig. 15B,E). I also detected fewer EsxA+ cells on transwells with SR-B1 shRNA expressing HBE cells (Fig. 15B,F), implying loss of SR-B1 reduces EsxA binding to M cells in vitro. Additionally, the majority of the EsxA+ cells on transwells with non-targeting shRNA expressing HBE cells were positive for SR-B1 (Fig. 15A,G). Taken together, these data suggests that EsxA preferentially binds SR-B1 expressing M cells in vitro.

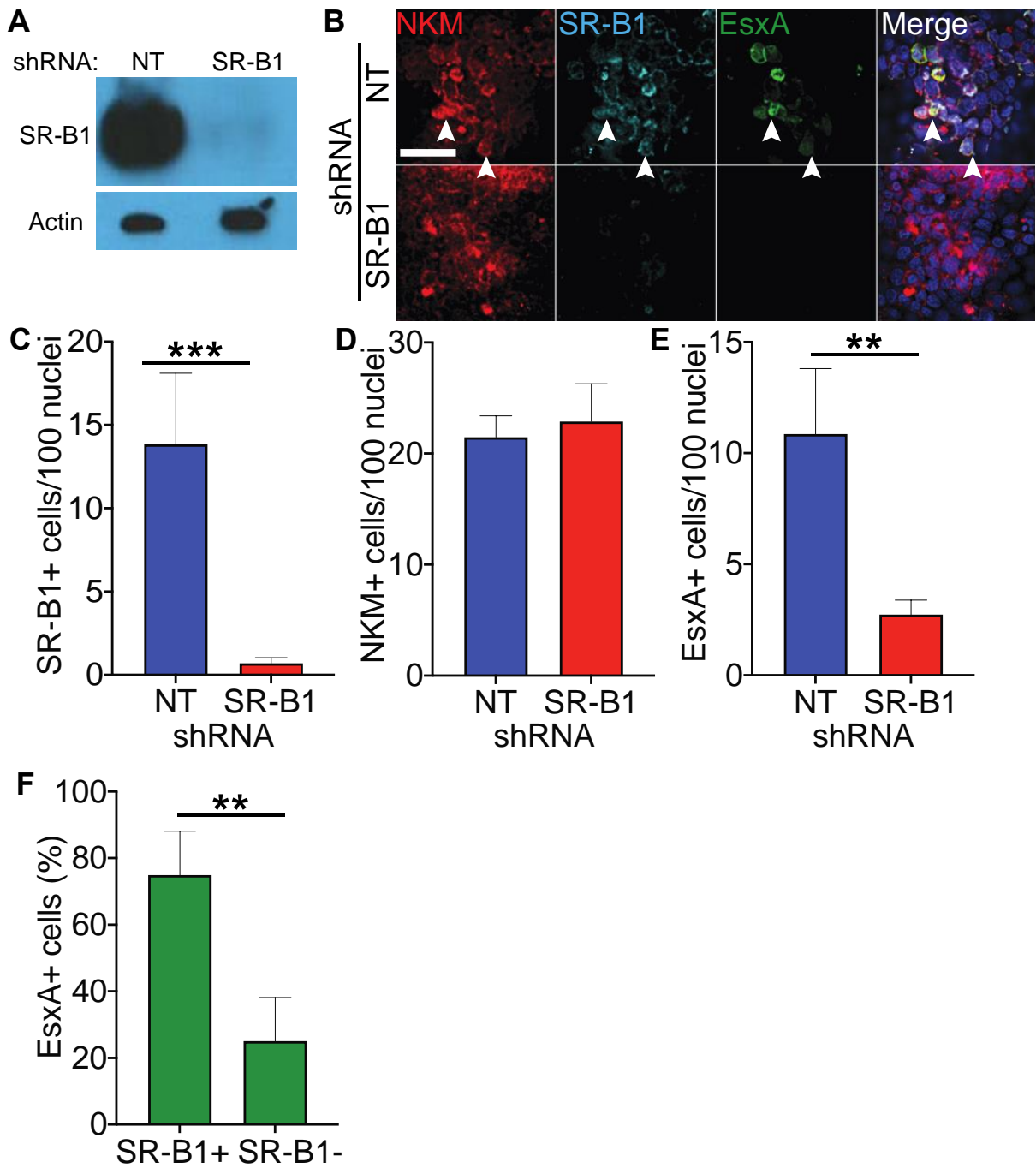


Figure 15. Loss of SR-B1 reduces EsxA binding to M cells in vitro. **A**, Western blot for SR-B1 (top) or beta-actin (bottom) of HBE cells expressing a non-targeting or SR-B1 targeting shRNA. Scale bar, 40 μ m. **B**, Raji B transwells with HBE cells expressing either the non-targeting or SR-B1 shRNA were incubated with biotinylated EsxA and stained with NKM 16-2-4 (red), anti-SR-B1 (cyan), and Alexa Fluor 488 conjugated streptavidin (green). Arrows denote examples of triple positive cells. **C,D,E**, The number of NKM positive cells (**C**), SR-B1 positive cells (**D**), and EsxA positive cells (**E**) on transwells described from **B** were quantified using ImageJ. **F**, The percentage of SR-B1+ and SR-B1- EsxA positive cells from Raji B transwells with non-targeting shRNA expressing HBE cells was quantified using ImageJ. **p<0.01, ***p<0.001 as determined by Student's T test.

Loss of SR-B1 reduces Mtb binding and translocation in vitro

I next examined the role of SR-B1 in the ability of Mtb to bind to and translocate across M cells in vitro. shRNA expressing HBE cells were co-cultured with Raji B cells and infected with mCherry Mtb at 4°C to prevent internalization. Transwells were either fixed and analyzed by confocal microscopy (Fig. 16A,B) or lysed to enumerate bacterial CFU (Fig. 16C). In either case, I observed a reduction in Mtb binding on transwells with SR-B1 shRNA expressing HBE cells. I next co-cultured shRNA expressing HBE cells with RajiB cells and infected transwells with Mtb at 37°C for one hour and measured translocation to the basal compartment. I observed a reduction in bacterial translocation across transwells with SR-B1 shRNA expressing HBE cells (Fig. 16D) with no change in the transwell TEER (Fig. 16E). Taken together, these data suggest that loss of SR-B1 reduces Mtb binding to and translocation across M cells in vitro.

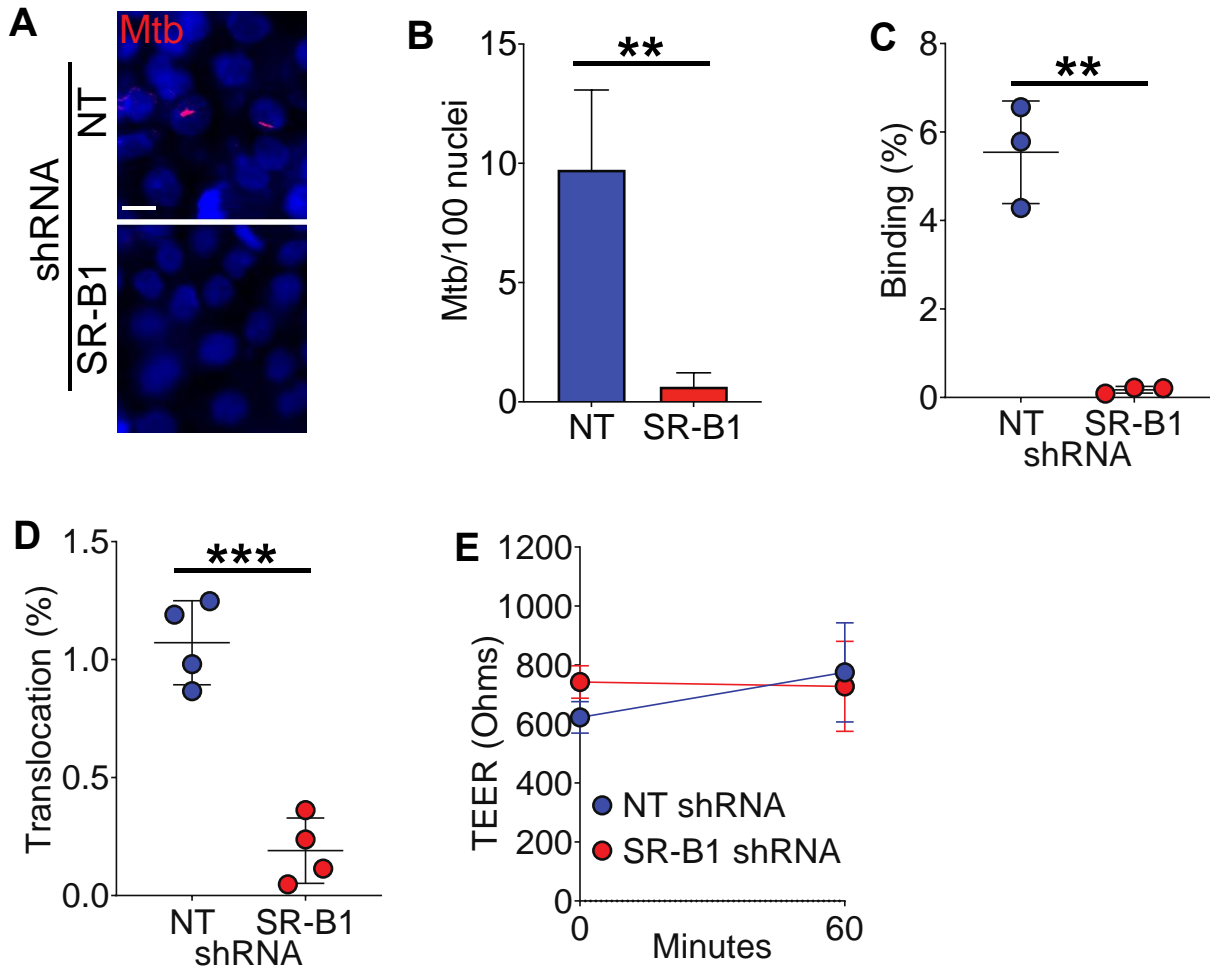


Figure 16. Loss of SR-B1 reduces Mtb binding and translocation in vitro. **A**, Raji B treated transwells with HBE cells expressing either the non-targeting or SR-B1 shRNA were incubated with mCherry Mtb, fixed, and analyzed by confocal microscopy. Scale bar, 10 μ m. **B**, ImageJ was used to quantify the number of bound bacteria from the transwells in **A**. **C**, Raji B transwells with HBE cells expressing either the non-targeting or SR-B1 shRNA were incubated with WT Mtb, washed, and then lysed. Percent binding was calculated by comparing bacterial CFU with the

initial inoculum. **D,E**, WT Mtb were added to the apical chamber of Raji B treated transwells with HBE cells expressing either the non-targeting or SR-B1 shRNA. Percent translocation was determined by comparing the bacterial CFU from the basal compartment after 60 minutes with the inoculum (**D**) with the transwell TEER being measured before and after the experiment (**E**). ** $p < 0.01$, *** $p < 0.001$ as determined by Student's T test.

Discussion

Here I identify SR-B1 as an M cell receptor required for Mtb binding and translocation through M cells in vitro. SR-B1 is a highly glycosylated 57 kDa membrane receptor protein that binds high-density lipoprotein and mediates uptake of cholesterol esters [62]. SR-B1 is expressed mainly in the adrenal gland, placenta, liver, and ovary of adults with lower expression in macrophages and the gastrointestinal epithelium [62]. SR-B1 also binds ApoE to facilitate cholesterol uptake [66], which may explain the identification of ApoE as an enriched peptide following Caco-2 cell treatment with EsxA by the TriCEPS screen.

Using HBE cells, I identified the interaction of EsxA with both a 57 kDa form of SR-B1 and a larger 130 kDa form of SR-B1 by western blotting. While the predicted molecular weight of SR-B1 is approximately 57 kDa, SR-B1 is usually detected at approximately 80 kDa by SDS-PAGE due to multiple glycosylation sites [62]. As the 57 kDa band represents the unglycosylated form of SR-B1 and is therefore presumably not found on the cell surface, it is unclear how EsxA is able to associate with this form of SR-B1. It is possible that the EsxA:SR-B1 complex is endocytosed and that sugar residues on SR-B1 are removed in the endosomal compartment, leading to the smaller molecular weight band, although this remains to be tested. As mentioned previously, SR-B1 is predominately detected at approximately 82 kDa by SDS-PAGE. I have identified a larger band at approximately 130 kDa that represents the glycosylated form of SR-B1. While rare, this larger form of SR-B1 has also been

identified by other groups [67]. This size discrepancy may reflect an alternative glycosylation pattern or other post-translational modifications of SR-B1 in HBE cells as compared to other cell types. This could potentially be tested by purifying SR-B1 from HBE cells and comparing its mass spectrometric profile against SR-B1 from other cell types in order to understand the size discrepancy as observed by western blotting.

In addition to its role in cholesterol uptake, SR-B1 also has several roles in the innate immune system. SR-B1 binds bacterial products such as LPS, Gram-negative bacteria such as *Escherichia coli* and *Salmonella typhimurium* [68], Gram-positive bacteria such as *Staphylococcus aureus* and *Listeria monocytogenes* [69], mycobacteria including *Mycobacterium fortuitum* [65] and Mtb [36], viruses including hepatitis C virus [70], and eukaryotic pathogens including *Plasmodium falciparum* [71]. Due to its ability to bind disparate pathogens, it is tempting to consider SR-B1 as a multifunctional receptor used by the immune system for the detection and elimination of various pathogens. However, certain pathogens, including the hepatitis C virus, have evolved to use SR-B1 as a receptor for viral entry [71], clouding the role of SR-B1 as being beneficial only to the host. I therefore propose a similar model where SR-B1 is required for binding of Mtb to M cells in order to facilitate entry into the host.

CHAPTER FIVE Results

PRIMARY HUMAN AIRWAY M CELLS ARE PORTALS OF ENTRY FOR MTB IN A T7SS DEPENDENT MANNER

Introduction

We have previously shown that mice treated with an M cell depleting antibody survive longer after Mtb infection than mice treated with a control antibody [31], highlighting the importance of M cells in Mtb dissemination and disease in mice. However, as tuberculosis is primarily a human disease [72], my ultimate goal is to understand the role of M cells, SR-B1, and EsxA in the development of human tuberculosis. By determining the role of SR-B1 and EsxA in the development of lymphoid TB, it may be possible to develop novel vaccines or therapeutics to reduce this form of TB. Based off our in vitro and in vivo work, I hypothesize that primary human airway M cells are a portal of entry for Mtb. Here I show that primary human airway M cells have elevated expression of SR-B1 and are able to internalize Mtb in a T7SS dependent manner.

Results

SR-B1 is expressed preferentially by mouse and human airway M cells

I first verified my *in vitro* observation that M cells preferentially express SR-B1 as compared to other epithelial cells. I obtained sections of mouse NALT or human adenoids, both of which have been shown to contain M cells [28, 29]. I incubated tissue sections with NKM 16-2-4 and SR-B1 targeting antibodies and analyzed the staining by confocal microscopy. For both mouse NALT (Fig. 17A) and human adenoids (Fig. 17B), I identified sections of the epithelium that were NKM+. These sections also were positive for SR-B1 expression, verifying that SR-B1 is expressed by airway M cells *in vivo*. Importantly, I did not observe SR-B1 expression in regions of the epithelium that were NKM-, implying that SR-B1 is preferentially expressed by airway M cells as compared to other epithelial cells *in vivo*.

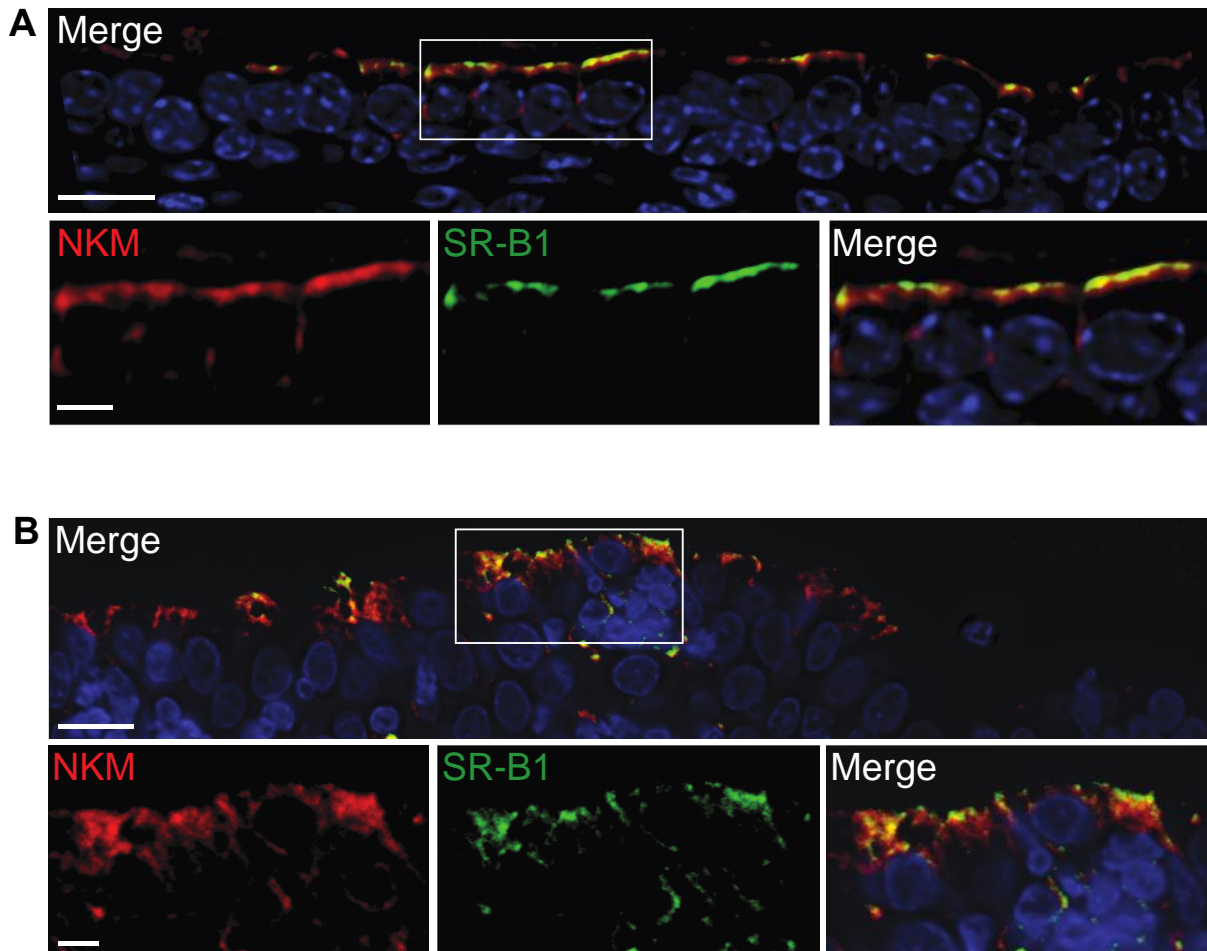


Figure 17. SR-B1 is expressed preferentially by mouse and human airway M cells in vivo. Mouse NALT sections (A) and human adenoid sections (B) were stained with NKM 16-2-4 and anti-SR-B1 antibodies and analyzed by confocal microscopy. Scale bar, 5 μm in top image of each set, 15 μm in bottom images of each set.

M cells from explanted human adenoids can be identified using flow cytometry

I utilized the human adenoid model to study primary airway M cells in vivo as tuberculosis is primarily a human disease and my ultimate goal was to gain a better understanding of the role of M cells, Mtb EsxA, and host SR-B1 in the context of Mtb infection. I first wanted to test if I could successfully disaggregate adenoids into a single cell suspension and analyze the cells by flow cytometry. I obtained human adenoids surgically removed from children as part of a treatment plan for sleep apnea. Adenoids were cut into small pieces, disaggregated into a single cell suspension, and incubated with PE conjugated NKM 16-2-4 and BV421 conjugated EpCAM, a marker for epithelial cells and analyzed by flow cytometry (Fig. 18A). I observed that roughly 10% of the adenoid was comprised of EpCAM+NKM-epithelial cells and roughly 1% of the adenoid was EpCAM+NKM+ M cells (Fig. 18B).

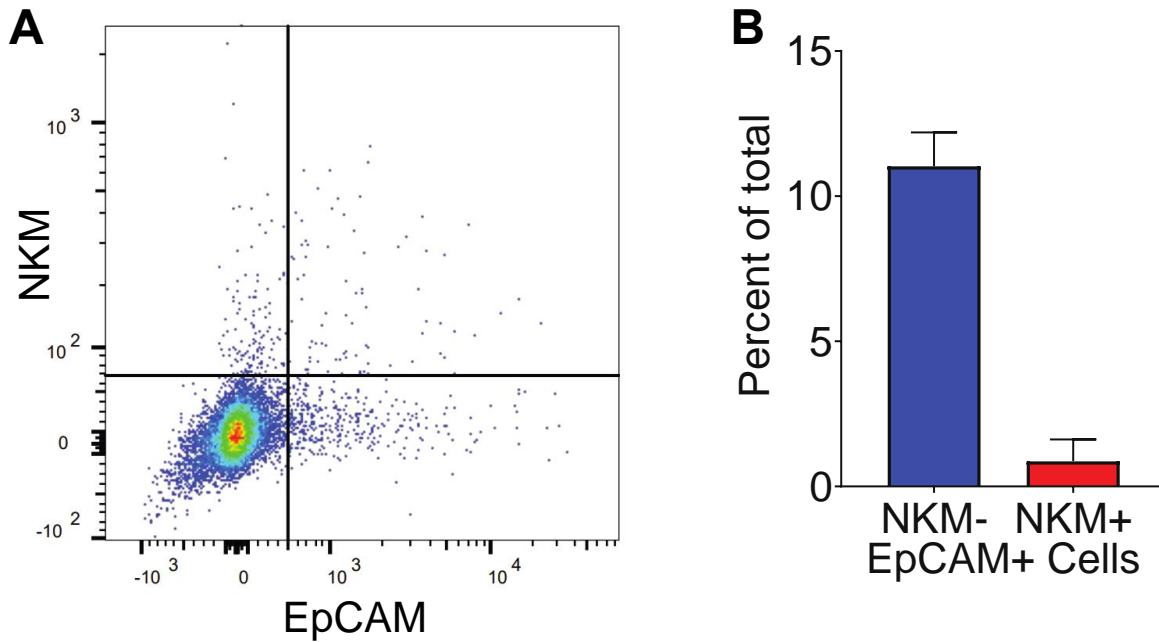


Figure 18. M cells from explanted human adenoids can be identified using flow cytometry. **A**, Adenoids were disaggregated into a single cell suspension, stained with PE-conjugated NKM 16-2-4 and BV421-conjugated anti-EpCAM, and analyzed by flow cytometry. **B**, The proportion of NKM-EpCAM⁺ and NKM⁺EpCAM⁺ cells were identified for six adenoids.

Primary human airway M cells have higher SR-B1 expression than neighboring epithelial cells

I next verified my microscopy findings that primary human airway M cells have higher SR-B1 expression as compared to other epithelial cells. I disaggregated adenoids into a single cell suspension and stained with both NKM 16-2-4 and EpCAM as described previously. Cells from the same donor were then incubated with either rabbit anti-SR-B1 or normal rabbit IgG followed by a fluorescently tagged secondary antibody (Fig. 19A-I). I observed significantly more SR-B1⁺ cells in the EpCAM⁺NKM⁺ compartment as compared to the EpCAM⁺NKM⁻ cells (Fig. 19J, right). This was not due to any inherent autofluorescence among these cells as there was no difference between the groups when the IgG control was used (Fig. 19J, left). Taken together, these data suggest that SR-B1 expression is higher on primary human airway M cells as compared to other epithelial cells.

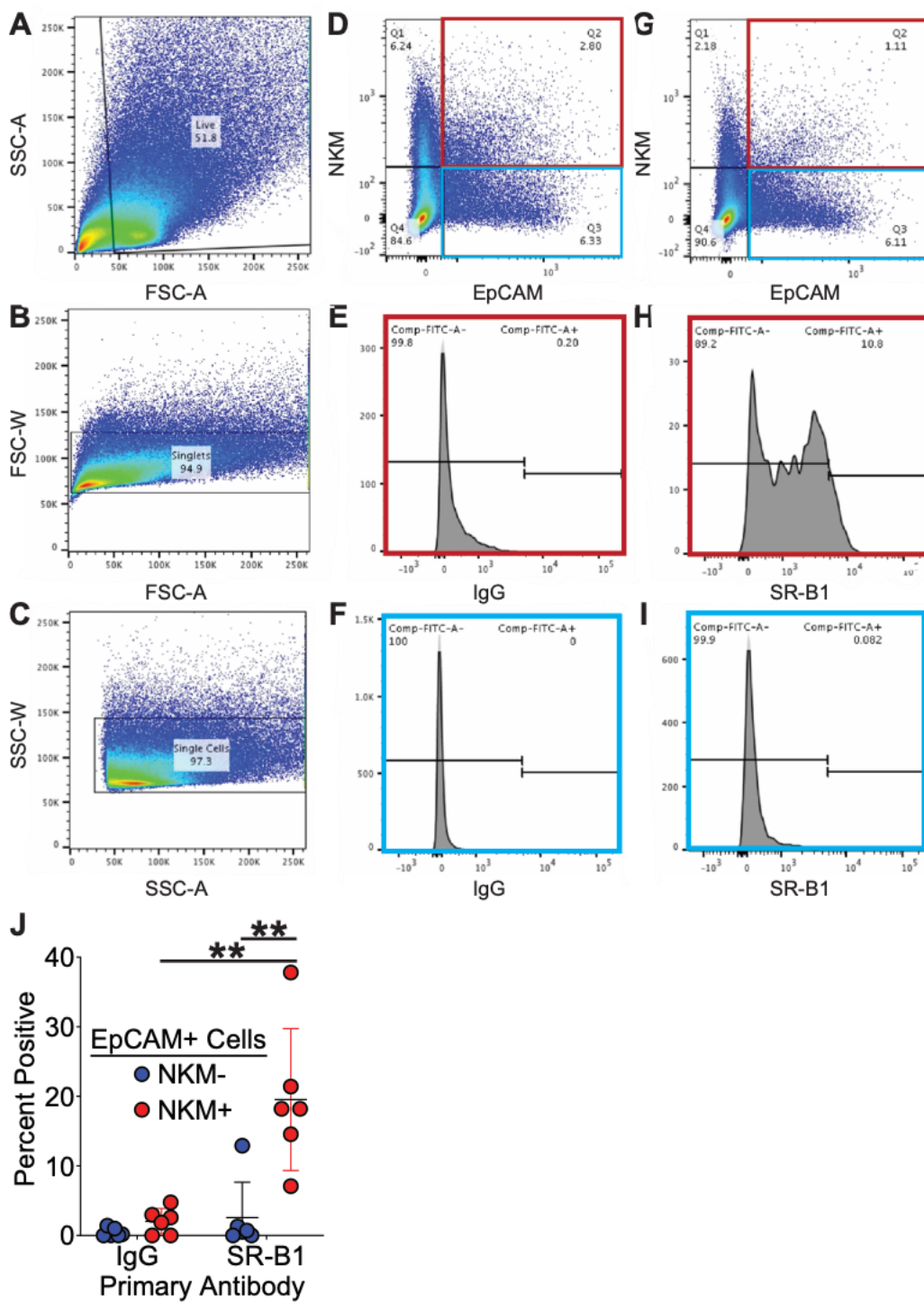


Figure 19. Primary human airway M cells have higher SR-B1 expression as compared to other epithelial cells. A-C, Gating strategy for unstained cells. Debris was excluded using FSC-A and SSC-A to yield the live cell population (**A**). Single cells were identified using the FSC-A and FSC-W (**B**) and singlets were identified using SSC-A and SSC-W (**C**). Gates for stained samples were established using unstained samples. **D-F,** Adenoids were stained with mouse BV421 conjugated anti-EpCAM, mouse PE conjugated NKM 16-2-4, or a rabbit IgG followed by a donkey-anti-rabbit 488 conjugated antibody. Using the gating strategy described in **A-C**, NKM⁺/EpCAM⁺ cells (highlighted in red) and NKM⁻/EpCAM⁺ cells (highlighted in blue) were analyzed for fluorescence in the green channel. **G-I** Adenoids were stained with mouse BV421 conjugated anti-EpCAM, mouse PE conjugated NKM 16-2-4, and rabbit anti-SR-B1 followed by a donkey-anti-rabbit 488 conjugated antibody. Using the gating strategy described in **A-C**, NKM⁺/EpCAM⁺ cells (highlighted in red) and NKM⁻/EpCAM⁺ cells (highlighted in blue) were analyzed for fluorescence in the green channel. **J,** Adenoids were disaggregated, stained with NKM 16-2-4 and anti-EpCAM antibodies as well as with either an anti-SR-B1 or an IgG control. The proportion of cells stained positively with the anti-SR-B1 or IgG antibody was determined for the NKM⁺EpCAM⁺ double positive cells and the NKM⁻EpCAM⁺ single positive cells. **p<0.01 as determined by the Wilcoxon matched pairs signed rank test.

Primary human airway M cells are a portal of entry for Mtb ex vivo

To test my hypothesis that human airway M cells could be a portal of entry for Mtb, each adenoid was sectioned into pieces. One section of an adenoid was infected with GFP Mtb with another section of the same adenoid treated with the vehicle control. Adenoid sections were then disaggregated, stained, and analyzed by flow cytometry to determine the proportion of GFP+ cells among either EpCAM+NKM+ cells or EpCAM+NKM- cells (Fig. 20A-I). I observed significantly more GFP+ cells for the EpCAM+NKM+ compartment as compared to the EpCAM+NKM- group (Fig. 20J), implying that Mtb utilizes M cells as a portal of entry.

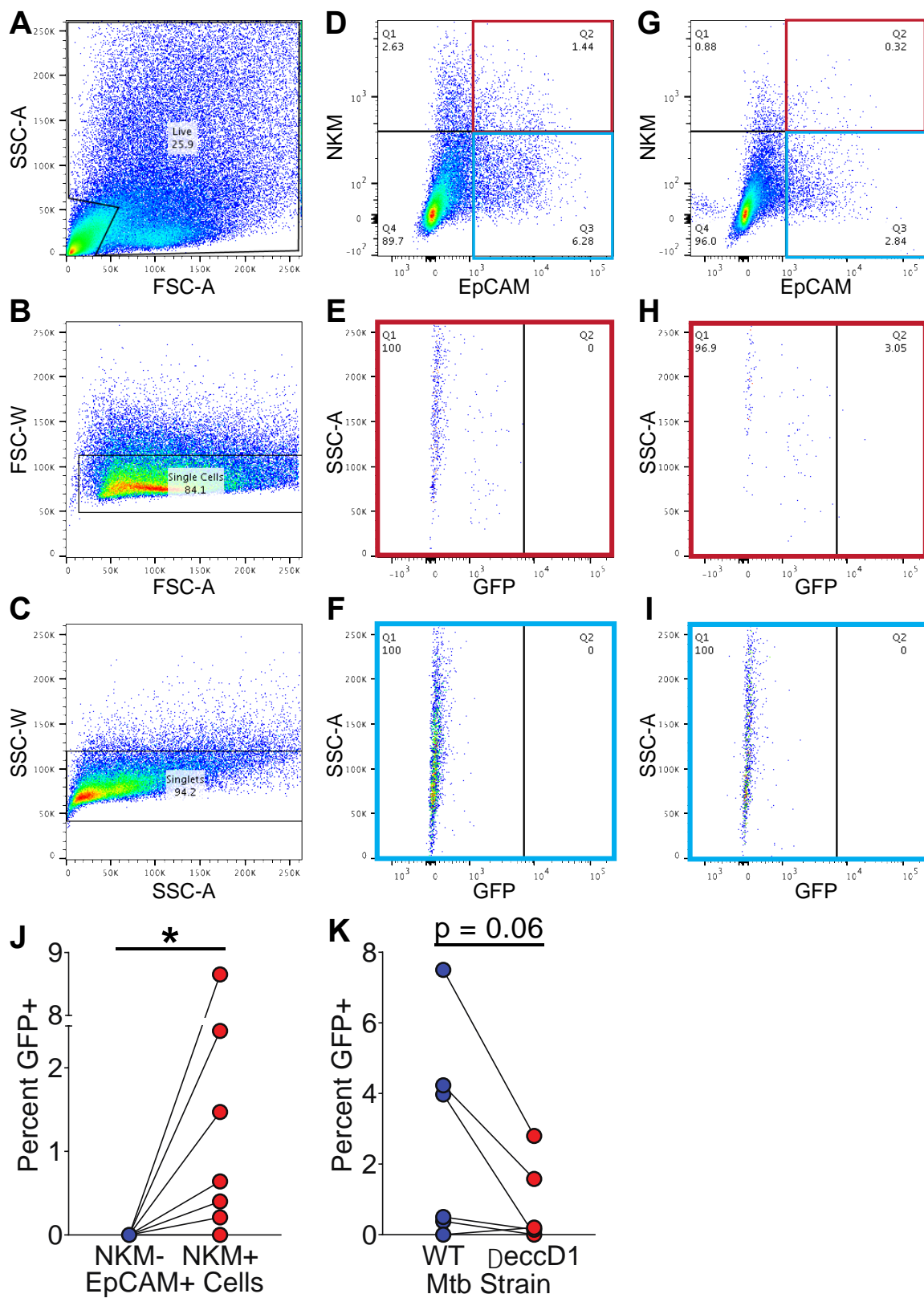


Figure 20. Primary human airway M cells are a portal of entry for Mtb ex vivo.

A-C, Gating strategy for unstained cells. Debris was excluded using FSC-A and SSC-A to yield the live cell population (**A**). Single cells were identified using the FSC-A and FSC-W (**B**) and singlets were identified using SSC-A and SSC-W (**C**). Gates for stained samples were established using unstained samples. **D-F**, Adenoids were infected with a vehicle control, disaggregated, and stained with mouse BV421 conjugated anti-EpCAM and mouse PE conjugated NKM 16-2-4. Using the gating strategy described in **A-C**, NKM⁺/EpCAM⁺ cells (highlighted in red) and NKM⁻/EpCAM⁺ cells (highlighted in blue) were analyzed for fluorescence in the green channel. **G-I**, Adenoids were infected with GFP Mtb, disaggregated, and stained with mouse BV421 conjugated anti-EpCAM and mouse PE conjugated NKM 16-2-4. Using the gating strategy described in **A-C**, NKM⁺/EpCAM⁺ cells (highlighted in red) and NKM⁻/EpCAM⁺ cells (highlighted in blue) were analyzed for fluorescence in the green channel. **J**, Human adenoids were infected with GFP⁺ Mtb, disaggregated, immunostained and analyzed by flow cytometry to determine the proportion of GFP⁺ Mtb containing NKM⁺/EpCAM⁺ and NKM⁻/EpCAM⁺ cells. Each line represents an adenoid from a separate donor. *p<0.05, Wilcoxon matched pairs signed rank test. **K**, Human adenoids were infected with GFP⁺ Mtb or GFP⁺ MtbΔ*eccD1*. The percentage of GFP⁺ Mtb containing NKM⁺/EpCAM⁺ double positive cells was determined by flow cytometry. Each line represents an adenoid from a separate donor. The Wilcoxon matched pairs signed rank test was used for comparison.

Uptake of Mtb by primary human airway M cells depends upon the Mtb T7SS

Finally, I tested my hypothesis that primary human airway M cell uptake of Mtb depends upon the Mtb T7SS. Adenoids were sectioned into pieces and infected with either GFP Mtb or GFP Mtb Δ eccD1. Specifically, one adenoid section was infected with GFP Mtb and another adenoid section from the same donor was infected with GFP Mtb Δ eccD1. Adenoid sections were then disaggregated, stained, and analyzed by flow cytometry to determine the proportion of GFP⁺ cells within the EpCAM⁺NKM⁺ compartment. I observed a trend towards significance between the two groups (Fig. 20K), implying that the T7SS is required for optimal uptake of Mtb.

Discussion

Here I show that primary human airway M cells have higher SR-B1 expression than neighboring epithelial cells. I also demonstrate that primary human airway M cells are able to internalize Mtb in a T7SS dependent manner. Intriguingly, the expression of SR-B1 on M cells greatly varied between donors. This difference in SR-B1 expression be due to age or race differences between donors. Alternatively, potential interactions between M cells and specific species within the oral microbiota may either promote or suppress SR-B1 expression on M cells, although this remains to be tested. Additionally, the range of internalization of Mtb into primary human airway M cells also greatly varied between donors. This could be explained by a number of factors, including differences in SR-B1 expression or polymorphisms in the region of the receptor required for bacterial binding . However, while the range of Mtb internalization varied between donors, I did not detect Mtb within other epithelial cells, data which is consistent with the idea that epithelial cells as a whole are largely inert to infection by Mtb [73]. Taken together, this data suggests that primary human airway M cells are a portal of entry for Mtb in in a T7SS dependent manner.

CHAPTER SIX

Conclusions and Recommendations

Summary of research findings

In this work, I used in vitro and in vivo M cell models to demonstrate a mucosal interaction between Mtb EsxA and the cell surface protein SR-B1. In vitro, Mtb lacking the T7SS failed to translocate across M cells, and in vivo, Mtb lacking the T7SS had a reduced ability to disseminate from the initial site of infection to regional lymph nodes, possibly due to a reduced ability to translocate across M cells. EsxA was sufficient to mediate translocation across M cells in vitro when conjugated to inert beads. Using an unbiased approach, I identified SR-B1 as a receptor for EsxA and verified this interaction using two epithelial cell lines. Within mucosal epithelia, SR-B1 is specifically expressed by human M cells in vitro, in mouse NALT and in human adenoids. Loss of SR-B1 reduced EsxA binding to M cells, and limited Mtb binding to and translocation across M cells in vitro. Finally, M cells were a portal of entry for Mtb in human adenoids in a T7SS dependent manner.

In mice, I observed that Mtb lacking the T7SS had a reduced ability to disseminate from the mouse NALT to the cervical lymph nodes, potentially due to a reduced ability to translocate across M cells. An alternative hypothesis for this observation centers on the observation that T7SS deficient strains of Mtb are

known to be attenuated in vivo and in macrophages [53], and the reduced CFU recovered from the draining lymph nodes could represent a macrophage survival defect as compared to WT Mtb. However, when I used a different attenuated Mtb strain for NALT infection, I observed a normal dissemination to the draining lymph nodes, suggesting that the reduced CFU recovered from cervical lymph nodes when mice were infected with Mtb lacking the T7SS was not simply due to an attenuation defect. In addition, the markedly reduced translocation of the T7SS deficient Mtb across M cells in vitro, in the absence of an innate immune response and over a very short time course, indicated that the T7SS was necessary for M cell mediated translocation.

Using an in vitro model of M cell development, I verified that the T7SS was required for Mtb to bind and translocate across M cells in vitro, implying that the T7SS may play a role in the ability of Mtb to attach to and translocate across epithelial cells. This finding is similar to other groups who showed that the H37Rv strain of Mtb crosses an epithelial monolayer consisting of A549 cells, a human alveolar cell line. However, this ability was absent in *Mycobacterium bovis* var BCG, a mycobacterial strain lacking T7SS among other virulence factors [74]. I observed that EsxA, a protein secreted through the T7SS, bound M cells in vitro, implying that EsxA may be an underappreciated adhesin for Mtb. EsxA has been previously shown to bind laminin, allowing for bacterial binding to the basal membrane of epithelial cells and subsequent lysis and escape [41]. In addition to laminin, other EsxA receptors that have been identified include β 2 microglobulin

and TLR-2 [42, 75]. However, I did not identify laminin, β 2 microglobulin or TLR-2 in my affinity purification assay, a discrepancy possibly related to the cell types used for binding experiments. Aside from protein binding, previous work has also implicated EsxA as a secreted pore-forming molecule [45], though this activity has recently been questioned [47]. In my transwell experiments utilizing recombinant EsxA, I observed no evidence of pore formation or epithelial damage. This could be due to the relatively short amount of time I incubated EsxA with my transwells for binding or translocation experiments. Alternatively, the pore forming properties of EsxA may only occur when the protein is in low pH conditions, such as in the lysosome.

Here I demonstrate an interaction of EsxA with SR-B1 using two epithelial cell lines. SR-B1 has been well characterized as a high-density lipoprotein receptor involved in cholesterol uptake [62]. It has also been shown that SR-B1 binds several bacterial molecules, including lipopolysaccharide and lipoteichoic acid produced by Gram-negative and Gram-positive bacteria respectively [69]. SR-B1 can also bind viral proteins, including glycoprotein E2 from the hepatitis C virus [76], and proteins from eukaryotic pathogens, such as the P36 protein from *Plasmodium vivax* [77]. For both HCV and *P. vivax*, recognition of SR-B1 on the host cell allows for pathogen invasion [76, 77]. Although direct interaction of EsxA and SR-B1 has not previously been shown, SR-B1 has been reported as a receptor for mycobacteria [36]. SR-B1 is sufficient for *Mycobacterium fortuitum* binding and internalization into HEK293 cells [65]. SR-B1 is also sufficient to

allow for Mtb binding to rat 6 fibroblast cells [36]. However, when wild-type or SR-B1^{-/-} C57/BL6 mice were infected with Mtb via the aerosol route, there was no difference in bacterial burden, granuloma size, cytokine secretion, or survival between the groups of mice within the first four months post-infection [36]. Based on our current data and previous results showing improved mouse survival during aerosol Mtb infection when M cells are reduced [31], I predict that loss of SR-B1 on M cells would reduce bacterial dissemination to draining mediastinal lymph nodes and promote a survival advantage for these mice as compared to WT mice. Unfortunately, SR-B1^{-/-} mice breed poorly and have cardiovascular defects [78], making them incompatible with such a study. Likewise, transgenic mice expressing an M-cell specific Cre have not been reported, preventing M cell specific deletion of *SR-B1*.

I also observed that adenoid M cells are a portal of entry for Mtb, which may have significant implications for Mtb pathogenesis in humans. Because respiratory MALT is more abundant in children than adults [79] and M cells are a key component of MALT [19], I propose that the increased incidence of extrapulmonary tuberculosis in children [80] is due to M cell mediated translocation. To that end, approaches towards interfering with the EsxA-SR-B1 interaction could prevent M cell mediated mucosal infection and protect against extrapulmonary tuberculosis. Interestingly, while some human adenoids showed a robust difference in M cell uptake between WT and T7SS deficient strains of Mtb, other adenoids showed little to no difference. This could be explained by a

variety of mechanisms. For example, it is possible that polymorphisms in the sequence of SR-B1 or differences in SR-B1 expression may increase or reduce binding of Mtb to M cells. Alternatively, there may be differences in the unique pattern recognition receptors (PRRs) expressed by M cells between different individuals. It is known that Mtb expresses a number of pathogen associated molecular patterns (PAMPs) that can be recognized by multiple PRRs [81]. Some individuals may show robust SR-B1 expression while other individuals may show upregulation of alternative, as-yet-unidentified receptors, explaining why some adenoids show less of a difference between the bacterial strains. A systematic comparison of cell surface receptor expression between in vitro human M cells, primary mouse M cells, and primary human M cells may help address this question.

In conclusion, I demonstrate that M cells are a portal of entry for Mtb in vitro, in mouse NALT, and in human adenoids. Utilizing mouse models and in vitro models, I identify EsxA and SR-B1 as a molecular synapse required for Mtb translocation across M cells in vitro and in vivo in both mice and humans. A greater understanding of the role of airway M cells in the context of infection by Mtb or other respiratory pathogens will yield insight into novel pathways with potential for new vaccine candidates or therapeutics.

Future directions

Determine the role of SR-B1 in uptake of Mtb by primary human airway M cells

My work has demonstrated that EsxA of Mtb can interact with SR-B1 expressed specifically by M cells in vitro leading to bacterial attachment and translocation across M cells. While I have demonstrated that the T7SS is necessary for bacterial translocation in vivo using primary human airway M cells, I have not demonstrated if this process requires SR-B1 in vivo. By identifying blocking reagents, such as neutralizing antibodies against SR-B1 or small molecule inhibitors of SR-B1, I can directly test what role SR-B1 has in the recognition and uptake of Mtb by primary human airway M cells.

Determine if EsxA homologues from other organisms interact with M cells in vitro

My work has demonstrated that Mtb EsxA is sufficient to mediate binding to and translocation across M cells in vitro. EsxA homologues are present in many clinically relevant organisms, such as *Staphylococcus aureus* and *Bacillus anthracis*. By cloning and purifying recombinant EsxA homologues from these species, I will be able to identify conserved regions required for EsxA binding. Additionally, I will be able to test if SR-B1 is also required for other bacterial species to translocate across M cells.

Determine mechanism for and consequence of Mtb uptake by M cells

My work has demonstrated that Mtb binds to SR-B1 on M cells to facilitate translocation across the epithelium. However, it is not clear through what

mechanism Mtb is internalized or trafficked. By treating my in vitro co-culture system with various uptake inhibitors, I may be able to identify pathways required for bacterial translocation. Additionally, it is currently unclear what effect uptake by or translocation across M cells has in terms of Mtb gene expression or if Mtb co-opts host membranes to create a protective barrier.

BIBLIOGRAPHY

1. Sauer, M.M., et al., *Catch-bond mechanism of the bacterial adhesin FimH*. Nat Commun, 2016. **7**: p. 10738.
2. Fennelly, K.P., et al., *Cough-generated aerosols of Mycobacterium tuberculosis: a new method to study infectiousness*. Am J Respir Crit Care Med, 2004. **169**(5): p. 604-9.
3. Fennelly, K.P. and E.C. Jones-Lopez, *Quantity and Quality of Inhaled Dose Predicts Immunopathology in Tuberculosis*. Front Immunol, 2015. **6**: p. 313.
4. Russell, D.G., C.E. Barry, 3rd, and J.L. Flynn, *Tuberculosis: what we don't know can, and does, hurt us*. Science, 2010. **328**(5980): p. 852-6.
5. Ehlers, S. and U.E. Schaible, *The granuloma in tuberculosis: dynamics of a host-pathogen collusion*. Front Immunol, 2012. **3**: p. 411.
6. Ai, J.W., et al., *Updates on the risk factors for latent tuberculosis reactivation and their managements*. Emerg Microbes Infect, 2016. **5**: p. e10.
7. Behr, M.A., P.H. Edelstein, and L. Ramakrishnan, *Revisiting the timetable of tuberculosis*. BMJ, 2018. **362**: p. k2738.
8. Pai, M., et al., *Tuberculosis*. Nat Rev Dis Primers, 2016. **2**: p. 16076.
9. Fontanilla, J.M., A. Barnes, and C.F. von Reyn, *Current diagnosis and management of peripheral tuberculous lymphadenitis*. Clin Infect Dis, 2011. **53**(6): p. 555-62.
10. Jones, C., et al., *Immunology and pathogenesis of childhood TB*. Paediatr Respir Rev, 2011. **12**(1): p. 3-8.
11. Wang, C., *An Experimental Study of Latent Tuberculosis*. The Lancet, 1916. **188**: p. 417-419.

12. Fox, G.J., M. Orlova, and E. Schurr, *Tuberculosis in Newborns: The Lessons of the "Lubeck Disaster" (1929-1933)*. PLoS Pathog, 2016. **12**(1): p. e1005271.
13. Lan, Z., M. Bastos, and D. Menzies, *Treatment of human disease due to Mycobacterium bovis: a systematic review*. Eur Respir J, 2016. **48**(5): p. 1500-1503.
14. Durr, S., et al., *Differences in primary sites of infection between zoonotic and human tuberculosis: results from a worldwide systematic review*. PLoS Negl Trop Dis, 2013. **7**(8): p. e2399.
15. Lerner, T.R., et al., *Lymphatic endothelial cells are a replicative niche for Mycobacterium tuberculosis*. J Clin Invest, 2016. **126**(3): p. 1093-108.
16. Ganchua, S.K.C., et al., *Lymph nodes are sites of prolonged bacterial persistence during Mycobacterium tuberculosis infection in macaques*. PLoS Pathog, 2018. **14**(11): p. e1007337.
17. Lin, P.L., et al., *Tumor necrosis factor neutralization results in disseminated disease in acute and latent Mycobacterium tuberculosis infection with normal granuloma structure in a cynomolgus macaque model*. Arthritis Rheum, 2010. **62**(2): p. 340-50.
18. Cesta, M.F., *Normal structure, function, and histology of mucosa-associated lymphoid tissue*. Toxicol Pathol, 2006. **34**(5): p. 599-608.
19. Corr, S.C., C.C. Gahan, and C. Hill, *M-cells: origin, morphology and role in mucosal immunity and microbial pathogenesis*. FEMS Immunol Med Microbiol, 2008. **52**(1): p. 2-12.
20. Ohno, H., *Intestinal M cells*. J Biochem, 2016. **159**(2): p. 151-60.
21. Hase, K., et al., *Uptake through glycoprotein 2 of FimH(+) bacteria by M cells initiates mucosal immune response*. Nature, 2009. **462**(7270): p. 226-30.

22. Beaulieu, J.F., *Differential expression of the VLA family of integrins along the crypt-villus axis in the human small intestine*. J Cell Sci, 1992. **102 (Pt 3)**: p. 427-36.
23. Clark, M.A., B.H. Hirst, and M.A. Jepson, *M-cell surface beta1 integrin expression and invasin-mediated targeting of Yersinia pseudotuberculosis to mouse Peyer's patch M cells*. Infect Immun, 1998. **66(3)**: p. 1237-43.
24. Nakato, G., et al., *New approach for m-cell-specific molecules screening by comprehensive transcriptome analysis*. DNA Res, 2009. **16(4)**: p. 227-35.
25. Nakato, G., et al., *Cutting Edge: Brucella abortus exploits a cellular prion protein on intestinal M cells as an invasive receptor*. J Immunol, 2012. **189(4)**: p. 1540-4.
26. Hellings, P., M. Jorissen, and J.L. Ceuppens, *The Waldeyer's ring*. Acta Otorhinolaryngol Belg, 2000. **54(3)**: p. 237-41.
27. Howie, A.J., *Scanning and transmission electron microscopy on the epithelium of human palatine tonsils*. J Pathol, 1980. **130(2)**: p. 91-8.
28. Karchev, T. and P. Kabakchiev, *M-cells in the epithelium of the nasopharyngeal tonsil*. Rhinology, 1984. **22(3)**: p. 201-10.
29. Date, Y., et al., *NALT M cells are important for immune induction for the common mucosal immune system*. Int Immunol, 2017. **29(10)**: p. 471-478.
30. Moyron-Quiroz, J.E., et al., *Role of inducible bronchus associated lymphoid tissue (iBALT) in respiratory immunity*. Nat Med, 2004. **10(9)**: p. 927-34.
31. Nair, V.R., et al., *Microfold Cells Actively Translocate Mycobacterium tuberculosis to Initiate Infection*. Cell Rep, 2016. **16(5)**: p. 1253-1258.
32. Brightbill, H.D., et al., *Host defense mechanisms triggered by microbial lipoproteins through toll-like receptors*. Science, 1999. **285(5428)**: p. 732-6.

33. Quesniaux, V.J., et al., *Toll-like receptor 2 (TLR2)-dependent-positive and TLR2-independent-negative regulation of proinflammatory cytokines by mycobacterial lipomannans*. J Immunol, 2004. **172**(7): p. 4425-34.
34. Schlesinger, L.S., *Macrophage phagocytosis of virulent but not attenuated strains of Mycobacterium tuberculosis is mediated by mannose receptors in addition to complement receptors*. J Immunol, 1993. **150**(7): p. 2920-30.
35. Schlesinger, L.S., et al., *Differences in mannose receptor-mediated uptake of lipoarabinomannan from virulent and attenuated strains of Mycobacterium tuberculosis by human macrophages*. J Immunol, 1996. **157**(10): p. 4568-75.
36. Schafer, G., et al., *The role of scavenger receptor B1 in infection with Mycobacterium tuberculosis in a murine model*. PLoS One, 2009. **4**(12): p. e8448.
37. Khan, A., et al., *Mesenchymal stem cells internalize Mycobacterium tuberculosis through scavenger receptors and restrict bacterial growth through autophagy*. Sci Rep, 2017. **7**(1): p. 15010.
38. Forrellad, M.A., et al., *Virulence factors of the Mycobacterium tuberculosis complex*. Virulence, 2013. **4**(1): p. 3-66.
39. Pym, A.S., et al., *Recombinant BCG exporting ESAT-6 confers enhanced protection against tuberculosis*. Nat Med, 2003. **9**(5): p. 533-9.
40. Lewis, K.N., et al., *Deletion of RD1 from Mycobacterium tuberculosis mimics bacille Calmette-Guerin attenuation*. J Infect Dis, 2003. **187**(1): p. 117-23.
41. Kinhikar, A.G., et al., *Potential role for ESAT6 in dissemination of M. tuberculosis via human lung epithelial cells*. Mol Microbiol, 2010. **75**(1): p. 92-106.
42. Sreejit, G., et al., *The ESAT-6 protein of Mycobacterium tuberculosis interacts with beta-2-microglobulin (beta2M) affecting antigen presentation function of macrophage*. PLoS Pathog, 2014. **10**(10): p. e1004446.

43. Simeone, R., et al., *Phagosomal rupture by Mycobacterium tuberculosis results in toxicity and host cell death*. PLoS Pathog, 2012. **8**(2): p. e1002507.
44. van der Wel, N., et al., *M. tuberculosis and M. leprae translocate from the phagolysosome to the cytosol in myeloid cells*. Cell, 2007. **129**(7): p. 1287-98.
45. Smith, J., et al., *Evidence for pore formation in host cell membranes by ESX-1-secreted ESAT-6 and its role in Mycobacterium marinum escape from the vacuole*. Infect Immun, 2008. **76**(12): p. 5478-87.
46. Raffetseder, J., et al., *Retention of EsxA in the Capsule-Like Layer of Mycobacterium tuberculosis Is Associated with Cytotoxicity and Is Counteracted by Lung Surfactant*. Infect Immun, 2019. **87**(3).
47. Conrad, W.H., et al., *Mycobacterial ESX-1 secretion system mediates host cell lysis through bacterium contact-dependent gross membrane disruptions*. Proc Natl Acad Sci U S A, 2017. **114**(6): p. 1371-1376.
48. Refai, A., et al., *Two distinct conformational states of Mycobacterium tuberculosis virulent factor early secreted antigenic target 6 kDa are behind the discrepancy around its biological functions*. FEBS J, 2015. **282**(21): p. 4114-29.
49. Chen, J.M., et al., *Phenotypic profiling of Mycobacterium tuberculosis EspA point mutants reveals that blockage of ESAT-6 and CFP-10 secretion in vitro does not always correlate with attenuation of virulence*. J Bacteriol, 2013. **195**(24): p. 5421-30.
50. Secott, T.E., T.L. Lin, and C.C. Wu, *Mycobacterium avium subsp. paratuberculosis fibronectin attachment protein facilitates M-cell targeting and invasion through a fibronectin bridge with host integrins*. Infect Immun, 2004. **72**(7): p. 3724-32.
51. Fujimura, Y., *Functional morphology of microfold cells (M cells) in Peyer's patches--phagocytosis and transport of BCG by M cells into rabbit Peyer's patches*. Gastroenterol Jpn, 1986. **21**(4): p. 325-35.

52. Teitelbaum, R., et al., *The M cell as a portal of entry to the lung for the bacterial pathogen Mycobacterium tuberculosis*. Immunity, 1999. **10**(6): p. 641-50.
53. Stanley, S.A., et al., *Acute infection and macrophage subversion by Mycobacterium tuberculosis require a specialized secretion system*. Proc Natl Acad Sci U S A, 2003. **100**(22): p. 13001-6.
54. de Jonge, M.I., et al., *ESAT-6 from Mycobacterium tuberculosis dissociates from its putative chaperone CFP-10 under acidic conditions and exhibits membrane-lysing activity*. J Bacteriol, 2007. **189**(16): p. 6028-34.
55. Abdallah, A.M., et al., *Type VII secretion--mycobacteria show the way*. Nat Rev Microbiol, 2007. **5**(11): p. 883-91.
56. Kerneis, S., et al., *Conversion by Peyer's patch lymphocytes of human enterocytes into M cells that transport bacteria*. Science, 1997. **277**(5328): p. 949-52.
57. Beloqui, A., et al., *A human intestinal M-cell-like model for investigating particle, antigen and microorganism translocation*. Nat Protoc, 2017. **12**(7): p. 1387-1399.
58. Nochi, T., et al., *A novel M cell-specific carbohydrate-targeted mucosal vaccine effectively induces antigen-specific immune responses*. J Exp Med, 2007. **204**(12): p. 2789-96.
59. Zacharia, V.M., et al., *cor, a novel carbon monoxide resistance gene, is essential for Mycobacterium tuberculosis pathogenesis*. MBio, 2013. **4**(6): p. e00721-13.
60. Brodin, P., et al., *Functional analysis of early secreted antigenic target-6, the dominant T-cell antigen of Mycobacterium tuberculosis, reveals key residues involved in secretion, complex formation, virulence, and immunogenicity*. J Biol Chem, 2005. **280**(40): p. 33953-9.
61. Frei, A.P., et al., *Ligand-based receptor identification on living cells and tissues using TRICEPS*. Nat Protoc, 2013. **8**(7): p. 1321-36.

62. Shen, W.J., S. Azhar, and F.B. Kraemer, *SR-B1: A Unique Multifunctional Receptor for Cholesterol Influx and Efflux*. *Annu Rev Physiol*, 2018. **80**: p. 95-116.
63. Dieudonne, A., et al., *Scavenger receptors in human airway epithelial cells: role in response to double-stranded RNA*. *PLoS One*, 2012. **7**(8): p. e41952.
64. Doench, J.G., et al., *Optimized sgRNA design to maximize activity and minimize off-target effects of CRISPR-Cas9*. *Nat Biotechnol*, 2016. **34**(2): p. 184-191.
65. Philips, J.A., E.J. Rubin, and N. Perrimon, *Drosophila RNAi screen reveals CD36 family member required for mycobacterial infection*. *Science*, 2005. **309**(5738): p. 1251-3.
66. Bultel-Brienne, S., et al., *Lipid free apolipoprotein E binds to the class B Type I scavenger receptor I (SR-BI) and enhances cholesteryl ester uptake from lipoproteins*. *J Biol Chem*, 2002. **277**(39): p. 36092-9.
67. Ganesan, L.P., et al., *Scavenger receptor B1, the HDL receptor, is expressed abundantly in liver sinusoidal endothelial cells*. *Sci Rep*, 2016. **6**: p. 20646.
68. Vishnyakova, T.G., et al., *CLA-1 and its splicing variant CLA-2 mediate bacterial adhesion and cytosolic bacterial invasion in mammalian cells*. *Proc Natl Acad Sci U S A*, 2006. **103**(45): p. 16888-93.
69. Bocharov, A.V., et al., *Targeting of scavenger receptor class B type I by synthetic amphipathic alpha-helical-containing peptides blocks lipopolysaccharide (LPS) uptake and LPS-induced pro-inflammatory cytokine responses in THP-1 monocyte cells*. *J Biol Chem*, 2004. **279**(34): p. 36072-82.
70. Dubuisson, J., F. Helle, and L. Cocquerel, *Early steps of the hepatitis C virus life cycle*. *Cell Microbiol*, 2008. **10**(4): p. 821-7.
71. Yalaoui, S., et al., *Scavenger receptor B1 boosts hepatocyte permissiveness to Plasmodium infection*. *Cell Host Microbe*, 2008. **4**(3): p. 283-92.

72. Brites, D. and S. Gagneux, *Co-evolution of Mycobacterium tuberculosis and Homo sapiens*. Immunol Rev, 2015. **264**(1): p. 6-24.
73. Reuschl, A.K., et al., *Innate activation of human primary epithelial cells broadens the host response to Mycobacterium tuberculosis in the airways*. PLoS Pathog, 2017. **13**(9): p. e1006577.
74. Bermudez, L.E., et al., *The efficiency of the translocation of Mycobacterium tuberculosis across a bilayer of epithelial and endothelial cells as a model of the alveolar wall is a consequence of transport within mononuclear phagocytes and invasion of alveolar epithelial cells*. Infect Immun, 2002. **70**(1): p. 140-6.
75. Pathak, S.K., et al., *Direct extracellular interaction between the early secreted antigen ESAT-6 of Mycobacterium tuberculosis and TLR2 inhibits TLR signaling in macrophages*. Nat Immunol, 2007. **8**(6): p. 610-8.
76. Heo, T.H., et al., *Hepatitis C virus E2 links soluble human CD81 and SR-B1 protein*. Virus Res, 2006. **121**(1): p. 58-64.
77. Manzoni, G., et al., *Plasmodium P36 determines host cell receptor usage during sporozoite invasion*. Elife, 2017. **6**.
78. Trigatti, B., et al., *Influence of the high density lipoprotein receptor SR-BI on reproductive and cardiovascular pathophysiology*. Proc Natl Acad Sci U S A, 1999. **96**(16): p. 9322-7.
79. Tschernig, T. and R. Pabst, *Bronchus-associated lymphoid tissue (BALT) is not present in the normal adult lung but in different diseases*. Pathobiology, 2000. **68**(1): p. 1-8.
80. Yang, Z., et al., *Identification of risk factors for extrapulmonary tuberculosis*. Clin Infect Dis, 2004. **38**(2): p. 199-205.
81. Stamm, C.E., A.C. Collins, and M.U. Shiloh, *Sensing of Mycobacterium tuberculosis and consequences to both host and bacillus*. Immunol Rev, 2015. **264**(1): p. 204-19.

